/

# A STUDY OF THE FEASIBILITY OF DESIGNING A SUPER-REGENERATIVE RECEIVER TO MEET CERTAIN CRITICAL REQUIREMENTS

Thaddeus Francis Kycia, B.Sc.

A thesis submitted to the Faculty of Graduate Studies and Research, McGill University, in partial fulfilment of the requirements for the degree of Master of Science.

## ABSTRACT

A super-regenerative receiver has been designed for linear mode operation in a band from 455 Mc./sec. to 510 Mc./sec. For linear mode operation it was necessary to use automatic gain stabilization, which also kept the oscillator output pulses at a steady amplitude. The receiver was constructed, having a band-width of 630 Kc./sec and a noise figure of 20 db. The experimental results were in good agreement with the theoretical estimates, and numerical values for comparison are provided wherever possible.

The receiver can detect a minimum signal of 1.5 $\mu$volts, and it therefore more than meets the sensitivity requirements for use as a detector in a $\mu$.h.f. "bridge".

ACKNOWLEDGEMENTS

The writer wishes to express his appreciation to Dr. J.R. Whitehead who originated the project and under whose direction it was carried out; to Dr. H. G. I. Watson for allowing the use of his laboratory equipment and workshop, and to Mr. W. Avarlaid, Mr. B. Meunier, Mr. M. Kingsmill, and the staff of the Physics building for their kind cooperation.

Special thanks are due to Dr. T. W. R. East for his frequent assistance and advice during both the project and the writing of this thesis.

The writer is also indebted to the Defence Research Board, whose financial assistance made this work possible.

## FIGURES

CONTENTS

# 1. INTRODUCTION

## 1.1 History of Super-regenerative receivers

The principle of the super-regenerative oscillator was first introduced by E.H. Armstrong in 1922. Its high gain was realized, but its other remarkable features were overlooked and it was only thirteen years later that further investigation was pursued into the subject. H. Ataka, 1935; M.G. Scroggie, 1936 and F.W. Frink, 1938 published papers explaining the phenomenon of super-regeneration. At about the same time several unique circuits, making use of super-regeneration, appeared in print.

W.B. Lewis and C.J.A. Milner (1936) designed a duplex operation transceiver (simultaneous two way communication) by making use of the reradiating properties inherent in the super-regenerative oscillator. It acted alternatively as a receiver and transmitter during each quench period. Each transceiver would be sensitive to in-coming pulses at that specific time when the signal pulse just arrived from the other transceiver.

S. Becker and L.M. Leeds (1936) described a two way police radio system. This radio installation consisted of duplex operation from headquarters to each car and simplex operation between the cars. The receiver had a combination of both the super-regenerative and superheterodyne principles and the resultant sensitivity was more than sufficient to fulfill the rigorous requirements.

The super-regenerative circuit then found its way into numerous radio amateur receivers, as well as the "walkie talkie" developed by the U.S. Army Signal Corps and later modified for use during the Second World War. It had the desired features of being sensitive, light, simple and economical.

Other contributors who promoted the understanding of super-regenerative theory were W.E. Bradley (1948); A. Hazeltine; D. Richman and B.D. McLaughlin

(1948); Macfarlane and Whitehead (1946, 1948); H.A. Glucksman (1949) and L. Riebmann (1949).

The super-regenerative receiver became well known for its part in the wartime I.F.F. (identification friend or foe) Mark 111 responder, developed at T.R.E. in Great Britain. The purpose of the I.F.F. responder was to indicate to an observer at a radar station whether some distant aircraft was friendly. The responder on the allied aircraft would amplify the received radar pulses and reradiate them. These were picked up by the radar station and observed as long traces on the P.P.I. screen, compared to the small dots which represented the reflected pulses from an enemy aircraft. The use of a.g.s. (automatic gain stabilization) was made in these responders and this gave them the added feature of good stability over a wide frequency range (157-187Mc./sec.). More than 200,000 of these fully automatic responders were produced to be fitted into all the allied ships and planes as a joint effort by the United States and Great Britain.

"Super-Regenerative Receivers" by J.R. Whitehead (1950) describes the circuit of the Mark 111 responder, as well as many other circuits making use of the super-regenerative principle. The book also contains a comprehensive treatment of super-regenerative theory as well as physical interpretation of the results.

Another major piece of work published after that time on super-regenerative theory was by H.A. Wheeler in the form of two monographs on the analysis of super-regenerative selectivity and design formulas.

## 1.2 Purpose of the receiver

The object of the work undertaken was to study the feasibility of a super-regenerative receiver operating in the linear mode at 500Mc./sec., with specific properties which could make it useable as a "bridge" detector.

It would be used as a null indicator for a General Radio admittance meter. The specifications are that it would be able to detect 10 $\mu$v. of signal or better and that it would have a sufficient amount of stability. The particular receiver discussed here can detect 1.5 $\mu$v. of signal and achieves its very reliable operation through the use of the automatic gain stabilization. The purpose of the a.g.s. is to keep the receiver in the linear mode of operation, thus adding to the complexity of the receiver. On the whole, however, it is much simpler than a superheterodyne operating at the same frequency.

# 2. PRINCIPLE OF SUPER-REGENERATION

## 2.1 Super-regenerative action

A parallel tuned circuit can maintain oscillations if enough energy is supplied to it to overcome the resistive losses. If, at any time, more energy is supplied than dissipated, the oscillations will grow.

A positive feedback amplifier, which may consist of one tube, can be made to supply the necessary energy. The condition that oscillations be maintained is that the transconductance of the tube equal a certain value which depends on the losses in the circuit. The transconductance is a function of both the plate voltage and grid bias voltage. By periodically varying either of these, one can get the tube into a state where the oscillations grow, or where they decay. The general practice is to modulate the grid bias voltage with the output of a quench oscillator whose waveform, for simplicity, is sinusoidal. Over part of the quench cycle the grid bias is very negative and no oscillations exist. The grid then becomes less negative until it reaches the grid bias voltage, which is just necessary for oscillations to exist. The oscillations begin to grow as the bias becomes still less negative, until they reach a peak in amplitude which comes at a time when the grid bias returns to its critical value. Beyond that instant the oscillations decay and, under proper operating conditions, are well below noise at the time when the next cycle of build-up begins. The output of the super-regenerative oscillator is in the form of pulses at intervals equal to the period of the quench frequency.

## 2.2 The conductance cycle

There is an alternative method of stating the criterion for oscillations in a tuned circuit. In effect, the tuned circuit can be represented

by an induction capacitance and conductance, all in parallel. The conductance part of the circuit damps any oscillations that may be induced in it. The positive feedback amplifier, to which the tuned circuit is connected, acts like a negative conductance and, when the net resultant of the conductance across the tuned circuit is zero, the tube is in a state of steady oscillations. That is equivalent to saying that enough energy is being supplied to overcome the resistive losses. Besides acting as a negative conductance, the oscillator tube also has some small reactive effect, which causes a variation in the frequency of oscillation during the build-up cycle.

When the oscillations are growing, it indicates that the net conductance across the resonant circuit is negative. The net conductance varies directly as the transconductance of the tube which, in turn, varies as the grid bias voltage. The conductance cycle, as a function of time, can be obtained graphically by knowing the variations of the grid bias voltage with time.

A complete theory of the super-regenerative principle has been formulated in which use is made of the conductance cycle curve. A numerical example, showing how the experimental results compare with the theoretical formula, is illustrated in a later section.

## 2.3 Linear mode and a.g.s.

It was stated earlier that the super-regenerative (uhf) oscillator was to operate in the linear mode. Under that type of operation, amplitude modulation on the input signal is linearly reproduced by the output pulses. The requirements on the uhf oscillator are that the growing oscillations never reach saturation, if it is to operate in the linear mode.

The oscillations always start from noise and the signal induced in the oscillator at the input. If the oscillator had its mean D.C. bias so adjusted as to give adequate gain for low signal amplitudes, it would not require much

of an increase in signal amplitude to have the oscillations reaching saturation. Automatic gain stabilization is, therefore, necessary.

The detected output pulses are amplified and rectified by the a.g.s. system to give a negative D.C. voltage which controls the mean bias of the u.h.f. oscillator tube. Now, if a large signal is applied to the u.h.f. oscillator, the a.g.s. system makes the grid bias more negative, thus keeping the output pulses of the oscillator approximately constant.

## 2.4. General description of the receiver

A block diagram of the receiver is shown in figure 2.1. The output of the quench oscillator is at a frequency near 50 Kc./sec. and has a peak amplitude of about five volts under normal operating conditions.

The a.g.s. system consists of the amplifier, phase inverter and rectifier. The a.g.s. amplifier is tuned to quench frequency and so it responds only to the general frequency component of the detected pulses. Its output is, therefore, a quench frequency sine wave. The phase inverter, followed by a double diode detector, gives out the D.C. control voltage. This voltage provides the bias for the u.h.f. oscillator, thus completing the feedback loop.

The other rectifier, connected to the output of the phase inverter, gives out a positive output which is compared to an adjustable D.C. voltage by the microammeter. For this case, the meter is at the "Signal Strength Indicator" position, since changes in the output of the a.g.s. are caused by changes in the input signal amplitudes.

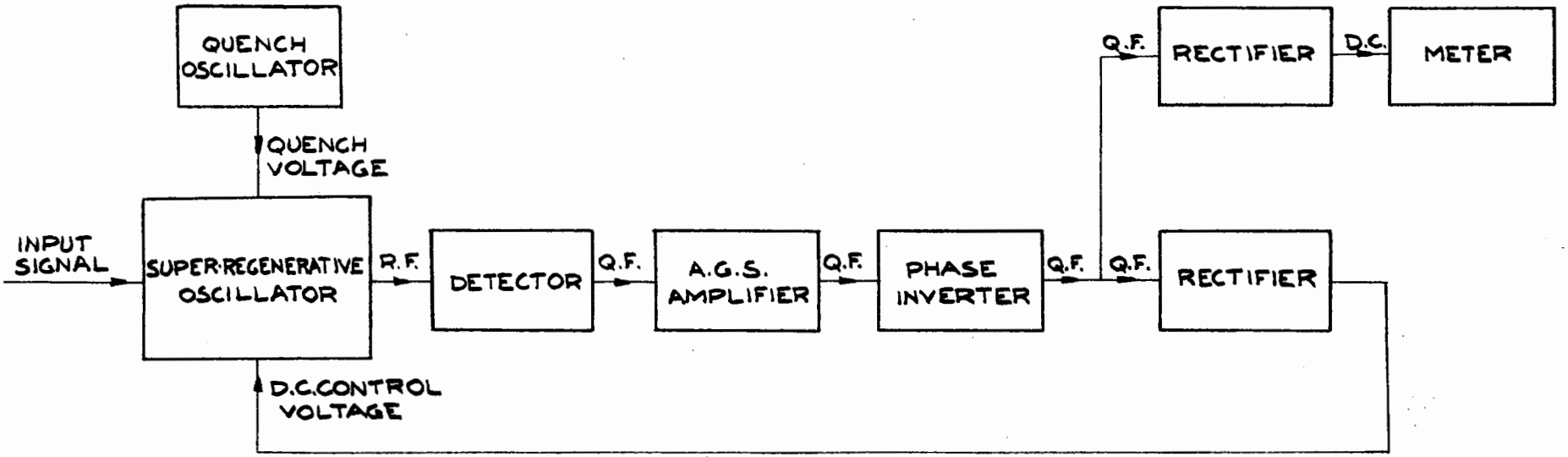


FIG. 2.1 BLOCK DIAGRAM OF THE SUPER-REGENERATIVE RECEIVER

## 3. The Super-Regenerative Oscillator

### 3.1 Construction of the oscillator

The cavity combination had been previously used in an u.h.f. amplifier and was converted into use for an oscillator by insulating the grid connection from the ground and fitting in a feedback loop. The oscillator, as shown in figure 3.1, consists of a tuned input cavity at the cathode and a tuned output cavity at the plate of the 5876 pencil triode.

The grid is grounded to u.h.f. oscillations through $C_3$ and $C_6$. $C_6$ consists of capacitance between the two sides of the flange holder and ground, polystyrene being the dielectric. $C_3$ has a value of 100 pf. and $C_6$ was determined from the parallel plate formula to have a value of 300 pf. The two capacitances add up to give 400 pf., which has an impedance of 0.75 ohms at 500 Mc./sec.

In actual practice, the two cavities are less than 1 cm. apart, the flange of the 5876 being the only part of the tube between the cavities. Both the cathode and plate of the tube fit into mounting blocks, which are capacitance-coupled to the quarter wave lines. By increasing the capacitance in the trimmers $C_1$ and $C_2$, the effective electrical length of the line is increased, thus decreasing the resonant frequency. The capacitance between the cathode and grid of the triode $V_1$ is given as 2.5 pf. This does not affect the electrical length of the line very much, since the cathode is coupled to it at the low impedance end. The plate, on the other hand, is coupled to the high impedance-end of the line and so the plate to grid capacitance of 1.4 pf. contributes much to the shortening of the line in the plate cavity, as is shown in fig. 3.1.

The oscillation frequency can be varied by means of $C_1$ and $C_2$ from 455 to 510 Mc./sec.

The input and output loops are situated at the low impedance, or high

# U.H.F. OSCILLATOR

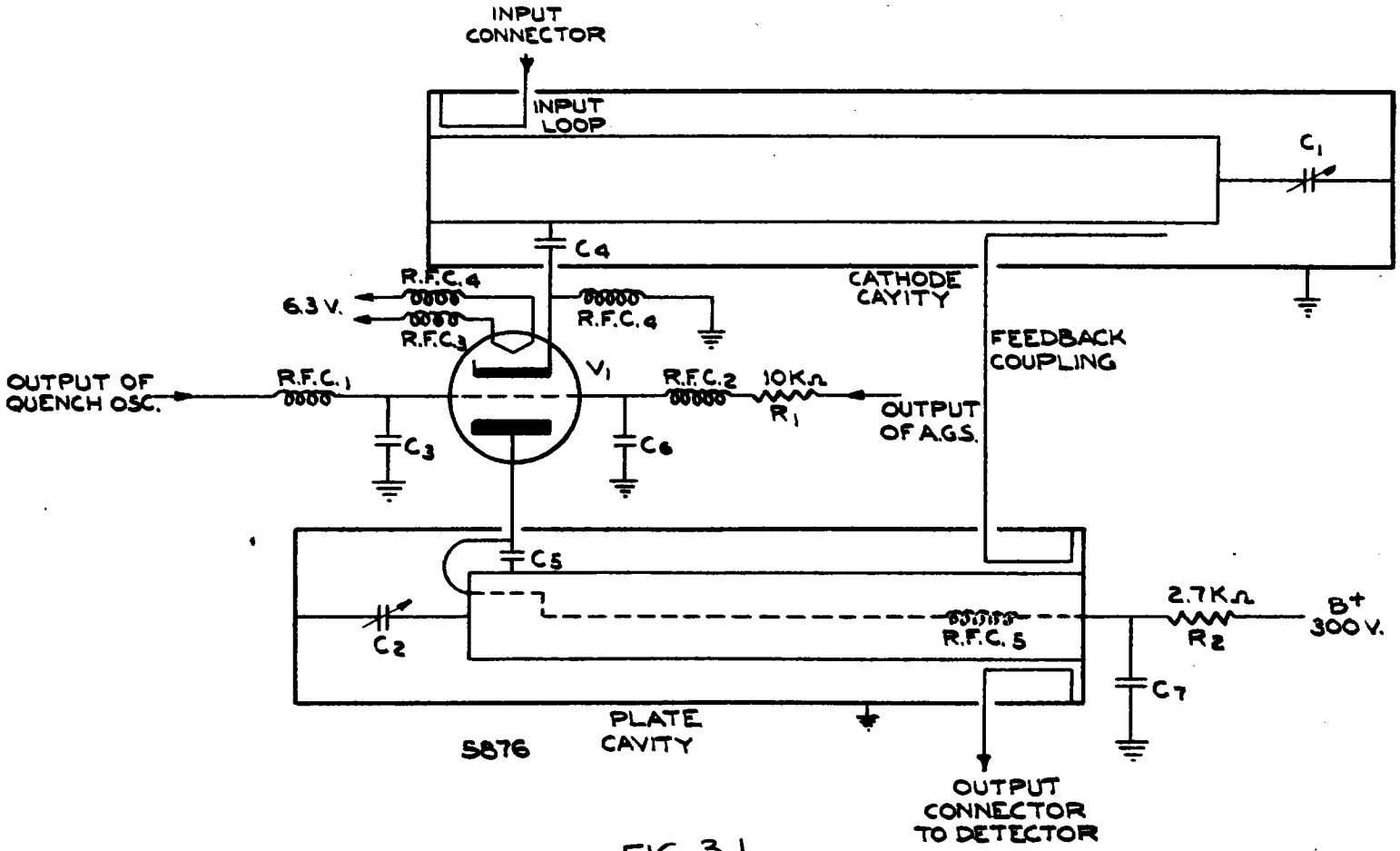


FIG. 3.1

# UHF OSCILLATOR

## List of Components

Cathode cavity

Plate cavity

$V_1$ 5876 u.h.f. High-Mu Triode

$C_1$, $C_2$ u.h.f. trimmers

Input loop

Output loop

Feedback coupling

$C_3$ 100 pf. ceramic condenser

$C_4$ coupling capacitance of 130 pf. to cathode cavity

$C_5$ coupling capacitance of 130 pf. to plate cavity

$C_7$ 0.05 $\mu$f.

$R_1$ 10K $\Omega$

$R_2$ 2.7K $\Omega$

R.F.C. 1 choke to quench oscillator

R.F.C. 2 choke to a.g.s.

R.F.C. 3, R.F.C. 4 chokes to heaters

R.F.C. 5 choke to cathode

R.F.C. 5 choke to plate

$C_6$ consists of capacitance, amounting to 300 pf. between the grid and the cavity through 0.25 cm of polystyrene insulation.

current ends of their respective cavities. The loops are coupled to the strong magnetic fields which exist at those ends. The feedback loop, on the other hand, is coupled to the magnetic field in the plate cavity and electric field in the cathode cavity. The electric field coupling is in the form of a capacitive probe.

Preliminary test showed that, at its best, the receiver could just detect five microvolts of input signal. This indicated that the input termination was weak and so the input loop was increased in size. The same type of loop was inserted at the output. After these modifications, it was evident from an observation of the low D.C. control voltage supplied by the a.g.s., that the new loops increased the loading on the cavities. To overcome this extra loading, the feedback loop was improved by lengthening the capacitive probe. Following this change, the D.C. control voltage went to its normal value. It was then found that the minimum detectable signal decreased to one and a half microvolts.

The super-regenerative gain in nepers is given as $\bar{a}/2C$ where $\bar{a}$ represents the integral with respect to time of the negative part of a conductance cycle and C is the equivalent capacitance of the plate cavity. One would then expect to have the gain of the receiver to increase with frequency , since C decreases and the corresponding D.C. control voltage from the a.g.s. to decrease the gain by an equal amount, by simply becoming more negative and thus decreasing $\bar{a}$. This was the case from 455 Mc./sec. to about 490 Mc./sec., after which the D.C. control voltage started becoming less negative as the frequency was increased to 510 Mc./sec. Since the 5876 can oscillate at a frequency as high as 1700 Mc./sec., it is quite justifiable to assume that the transit time of the 5876 would not cause such a large effect. The conclusion is that the efficiency of the feedback loop drops with increase in frequency

in the receiver band.

3.2 The 5876 pencil triode

The 5876 is a new tube developed only recently for u.h.f. frequencies and can be used as an oscillator up to 1700 Mc./sec. It has the features of minimum transit time, low cathode to plate capacitance, low lead inductance and good thermal stability. As much as 6 watts of energy can be dissipated at the plate if the plate cylinder should have a large surface of contact with its support.

The tube, when oscillating at 490 Mc./sec., dissipates at the plate 2.7 watts for no signal input, 1.5 watts for a large continuous wave signal of 0.5 volts and 6.0 watts if the grid should accidentally become grounded. If the oscillator should be detuned so that no oscillations exist, the plate dissipation would be 3.7 watts. The tube should not be allowed to dissipate more than 3.5 watts at the plate for any long length of time, since the polystyrene insulation for the plate support would weaken with the high rise in temperature.

## 3.3 Equivalent circuit of the plate cavity

In order to give a numerical example of the oscillation build-up and decay, it is first necessary to find an equivalent lumped resonant circuit for the plate cavity. An analagous lumped circuit of the oscillator is illustrated in fig. 3.2. No attempt is made to find the equivalent resonant circuit for the cathode cavity, since it does not enter the theory directly, but has some second order effects.

The line of the plate cavity can be represented by an inductance, a capacitance and a conductance, all in parallel, while the trimmer can be assumed to be an extra variable capacitance across the tuned circuit. Of the three unknowns, the capacitance and inductance arms will be first determined.

The trimmer acts like a parallel plate condenser with adjustable plate separation and air as a dielectric. The effective area of the plates was found to be 2.2 $cm^2$ and their separation was 0.10 cm. when the oscillator was tuned to 455 Mc./sec. ($f_1$). For an oscillator frequency of 480 Mc./sec. ($f_2$), the average separation was 0.18 cm. The capacitance of the parallel plate condenser is given by the expression 1.11 KA/4$\pi$d pf.,

where K is the dielectric constant and equals unity for air

A is the area of each plate in $cm^2$

d is the separation between the plates in cm. The formula gives a value of 1.95 pf. for 455 Mc./sec. and 1.08 pf. for 480 Mc./sec., the change in capacitance C thus being 0.87 pf. The value of the inductance L is found from the fundamental relation

$$L = \frac{1}{\Delta C}\left(\frac{1}{\omega_2^2} + \frac{1}{\omega_1^2}\right)$$

where $\omega_2 = 2\pi f_2$ , $\omega_1 = 2\pi f_1$

Substituting in the values

# ANALOGOUS LUMPED CIRCUIT OF THE U.H.F. OSCILLATOR

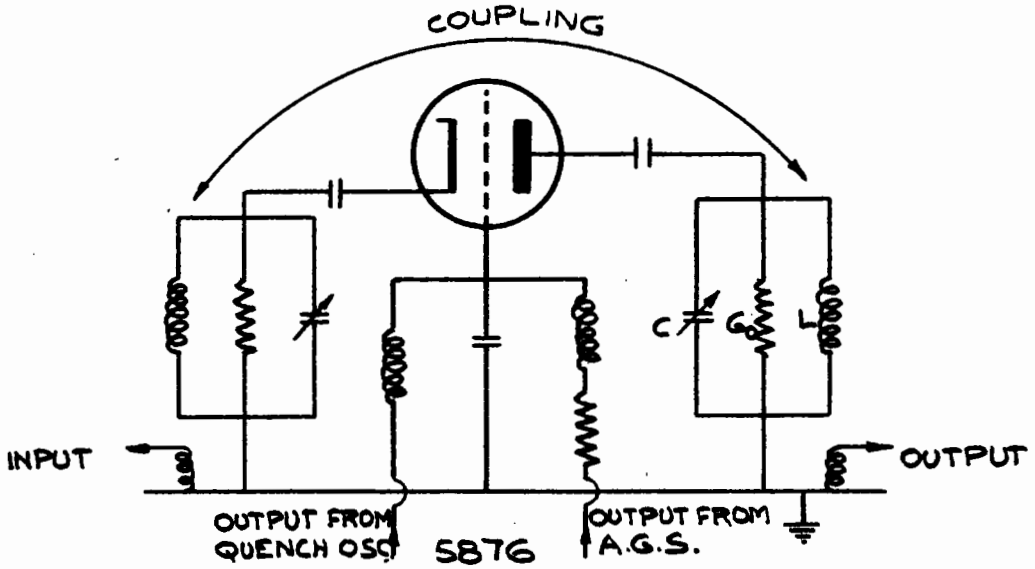


FIG. 3.2

$$L = \frac{1}{0.87\times10^{-12}}\left[\left(\frac{-1}{2\pi\times480\times10^{6}}\right)^{2}+\left(\frac{1}{2\pi\times455\times10^{6}}\right)^{2}\right]$$

$$= 0.0138\ \mu h.$$

For f = 488 Mc./sec. the equivalent capacitance $1/(2\pi f)^2$ is 7.7 pf. and for f = 500 Mc./sec., it is 7.4 pf. The next problem was to determine the equivalent conductance.

It is known that the bandwidth of a quiescent circuit is given by $b = \frac{G_o}{2\pi C}$ at - 3 db., where $G_o$ is the equivalent parallel conductance of the quiescent circuit. To find $G_o$ it is only necessary to measure b since C has already been calculated. The procedure was as follows:-

The power in the receiver was turned off while the output of the signal generator connected to the output loop of the receiver was increased to above 0.5 volts at 480 Mc./sec. The cathode cavity was detuned and the plate cavity tuned to 480 Mc./sec. For a fixed output of the signal generator, the detected portion, which was fed into a D.C. amplifier on an oscilloscope, gave an indication of the amount of off-resonance of the plate cavity from the signal generator frequency. At resonance the cavity absorbed little power and thus a larger output was observed on the C.R.T. When not in resonance, the impedance of the cavity, observed at the loop, decreased and so did the output voltage. The detector had been previously calibrated so that the frequency could be set to the values giving an output of 3 db. below resonance. The advantage of this method was that there were always large detected signals to be observed, even at -1 neper from resonance. The quiescent band-width obtained for the plate cavity was

$$b = 2.6 \text{ Mc./sec.} \quad \text{(at -3 db.)}$$

The equation for the conductance in parallel with the resonant circuit is then

$$G_o = 2\pi C\, b \qquad (3.4.1.)$$

$$= 129.\ \mu \text{ mhos.}$$

The equivalent circuit for the plate cavity is now approximately known.

3.4 The graphical determination of $a^-$

A graphic method for finding the value of $a^-$ under a particular set of conditions is described fully in Chapter 5 of "Super-Regenerative Receivers" by J.R. Whitehead. It is the most accurate method since it makes almost no use of approximations for the oscillator tube characteristic curves. As had been mentioned previously, $a^-$ is the integral with respect to time over a cycle of the negative part of the resonant circuit conductance G. The expression for G is

$$G = G_o - k\, g_m \qquad (3.4.2.)$$

where $G_o$ = quiescent conductance of the tuned circuit

$k$ = constant for given circuit conditions

$g_m$ = transconductance of the oscillator tube

From this equation it is apparent that when oscillations just start, G is zero and $g_m$ has its critical value $g_{mo}$. The expression for k is, therefore,

$$k = G_o/g_{mo} \qquad (3.4.3.)$$

The characteristic values of the quiescent circuit were

| | |
|---|---|
| Band-width | $b$ = 2.6 Mc./sec. (at-3db) |
| Capacitance | $C$ = 7.9 pf. |
| Resonant frequency | $f_o$ = 480 Mc./sec. |
| Shunt conductance | $G_o$ = 129 $\mu$ mhos. |

Other data consisted of

| | |
|---|---|
| Quench frequency | $f_q$ = 54 Kc./sec. |
| Quench amplitude | $A_q$ = 5.0 V |
| 5876 plate voltage | $V_a$ = 250 V |
| Output pulse peak | $V_1$ = 0.25 V |
| Input signal | $V$ = 12.5 $\mu$V |
| Bias for oscillations to begin | $V_{go}$ = - 3.4 V |
| Mean grid bias voltage | $V_{g^-}$ = - 7.4 V |

The transconductance $g_m$ grid bias voltage curve for the 5876 triode is not available in the published tube data and so it was necessary to obtain it experimentally. First, the plate current $I_a$ was recorded for different grid bias voltage values $V_g$, the plate being kept at 250 V. The results were plotted and shown in fig. 3.3. The slope of the curve $\Delta I_a/\Delta E_g$ which is defined as $g_m$ was then found for differenct $V_g$ values and similarly plotted in fig. 3.4. The required part of the transconductance ($g_m$) cycle can be seen in fig. 3.5. It is simply obtained by projecting the grid bias voltage as a function of time on the tube transconductance $g_m$ grid bias voltage, and getting the transconductance as a function of time. In the third quadrant is a 5 volt quench cycle superimposed on a -7.4 volt mean grid bias. In the first is the result, with the oscillatory region being above $g_{mo}$ = 3.5 m. mhos. corresponding to a grid bias of - 3.4 volts. The value k is now found from equation (3.4.2.) to be $0.037 \times 10^{-3}$.

Knowing this, the conductance cycle in fig. 3.6 is constructed from the transconductance cycle by using equation (3.4.3.). On the same figure is a grid bias voltage cycle showing from the conductance curve how the oscillator behaves during various parts of the quench period. The regenerative period, during which the input oscillations are amplified, is followed by the super-regenerative period, during which the oscillations grow rapidly. Then comes the damping period and the existing oscillations decay. The detected output pulse is also sketched from the trace on the oscilloscope, with its peak at the end of the super-regenerative period. The area a" was measured and found to be 105. $\mu$ mhos. $\mu$sec.

## 3.5 Theoretical formula for the output

Provided that several conditions are met, the expression for the oscillation amplitude across the plate cavity is given at any time t by

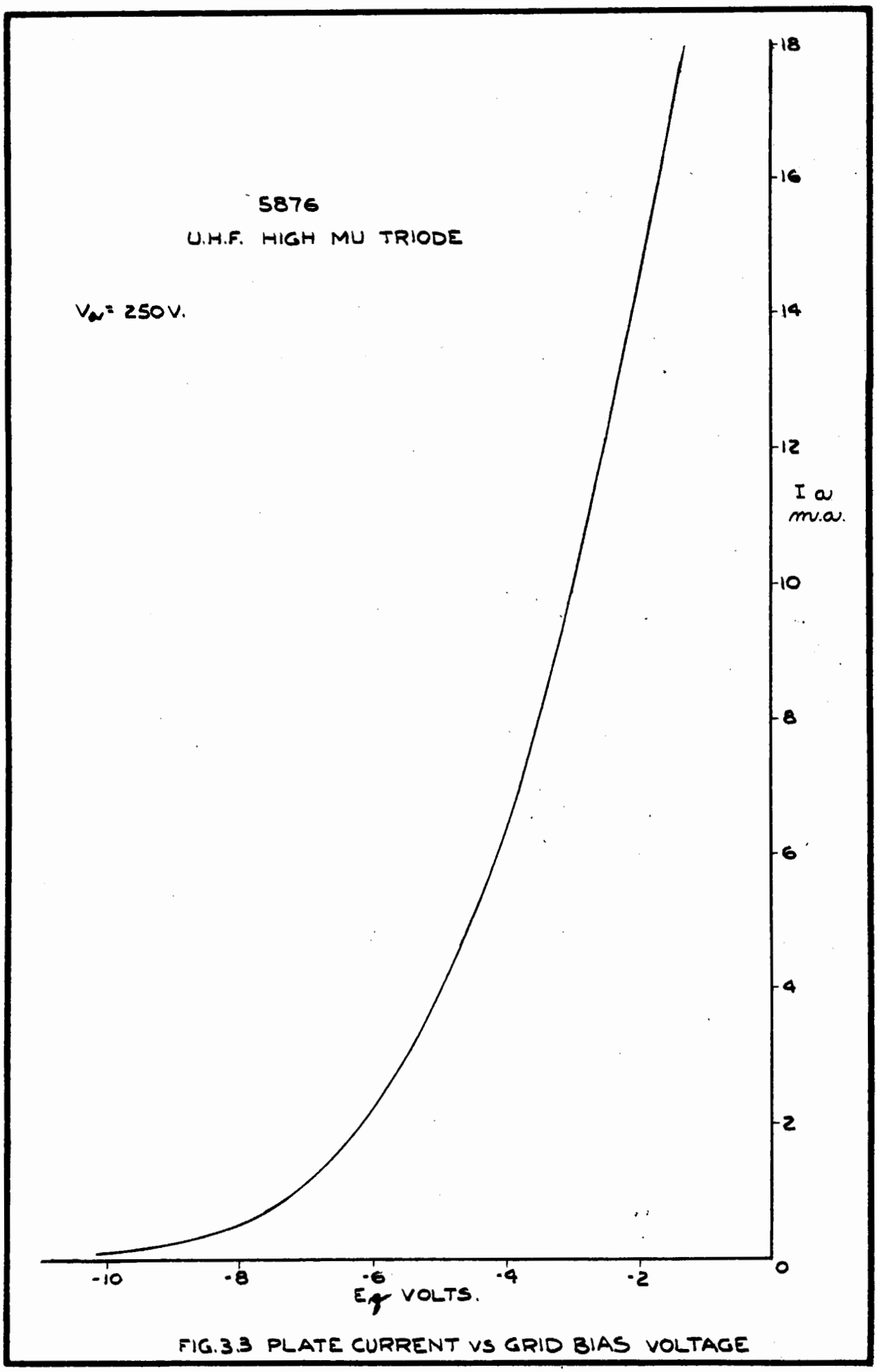


FIG. 3.3 PLATE CURRENT VS GRID BIAS VOLTAGE

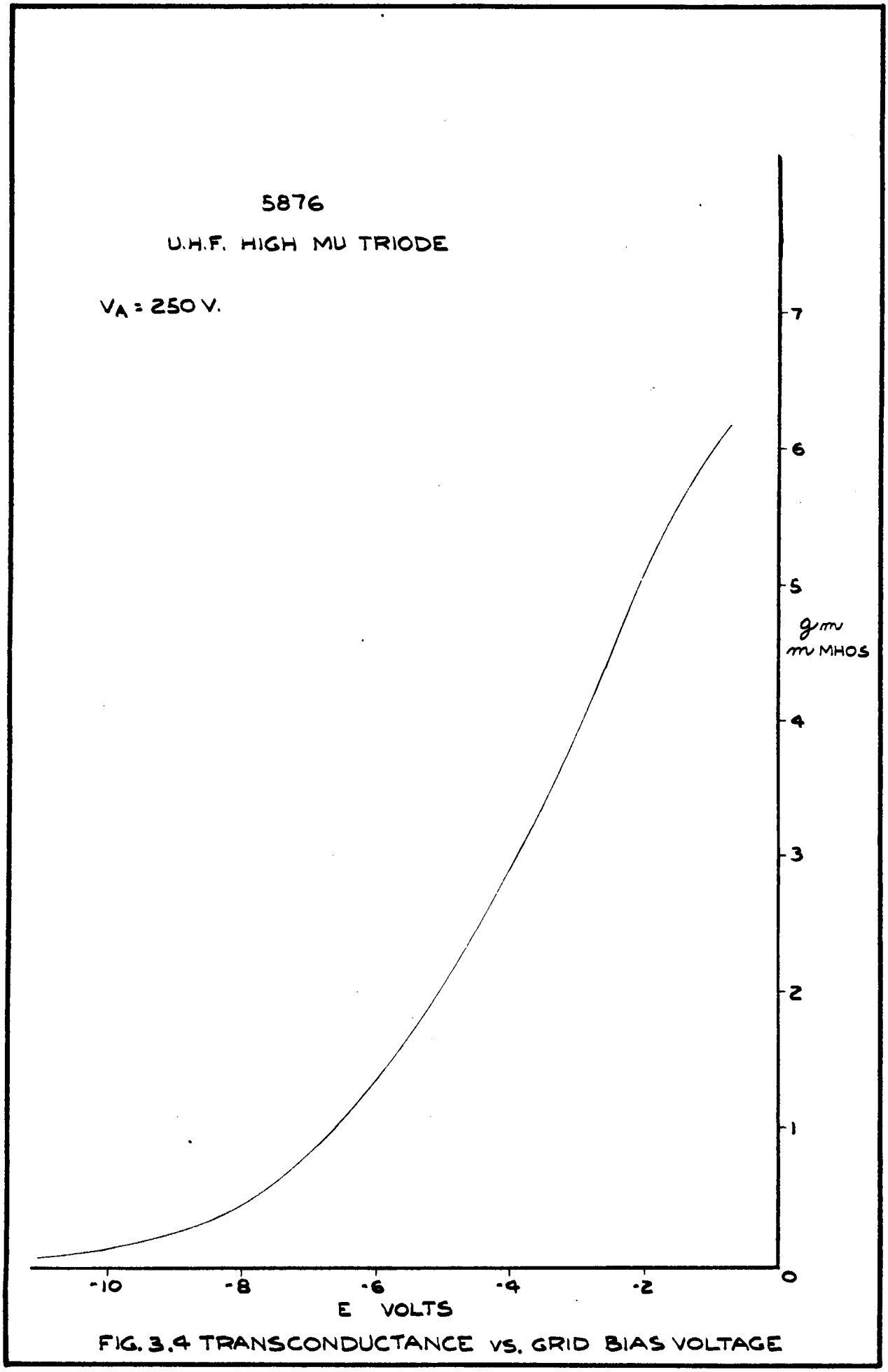


FIG. 3.4 TRANSCONDUCTANCE VS. GRID BIAS VOLTAGE

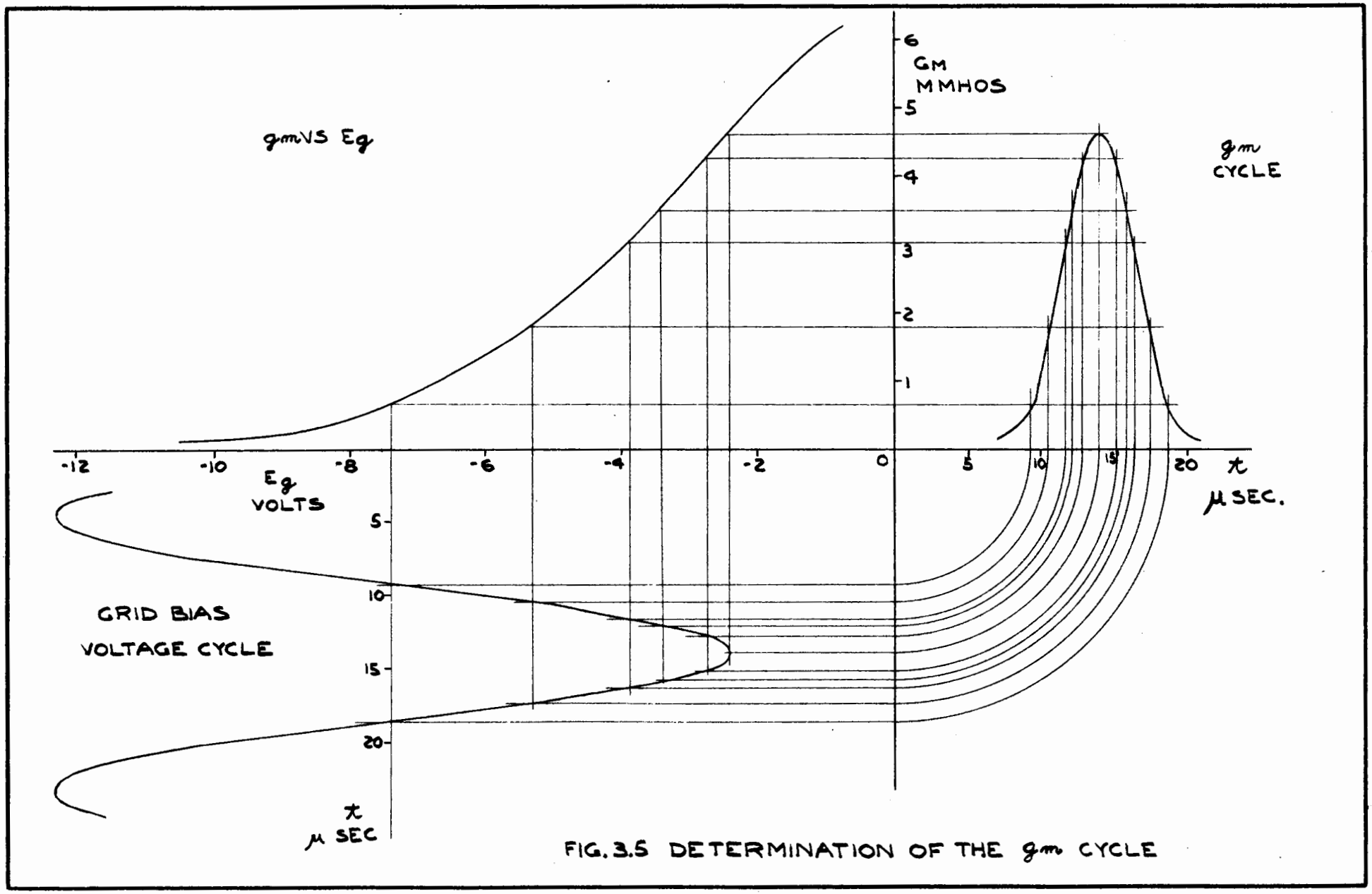


FIG. 3.5 DETERMINATION OF THE gm CYCLE

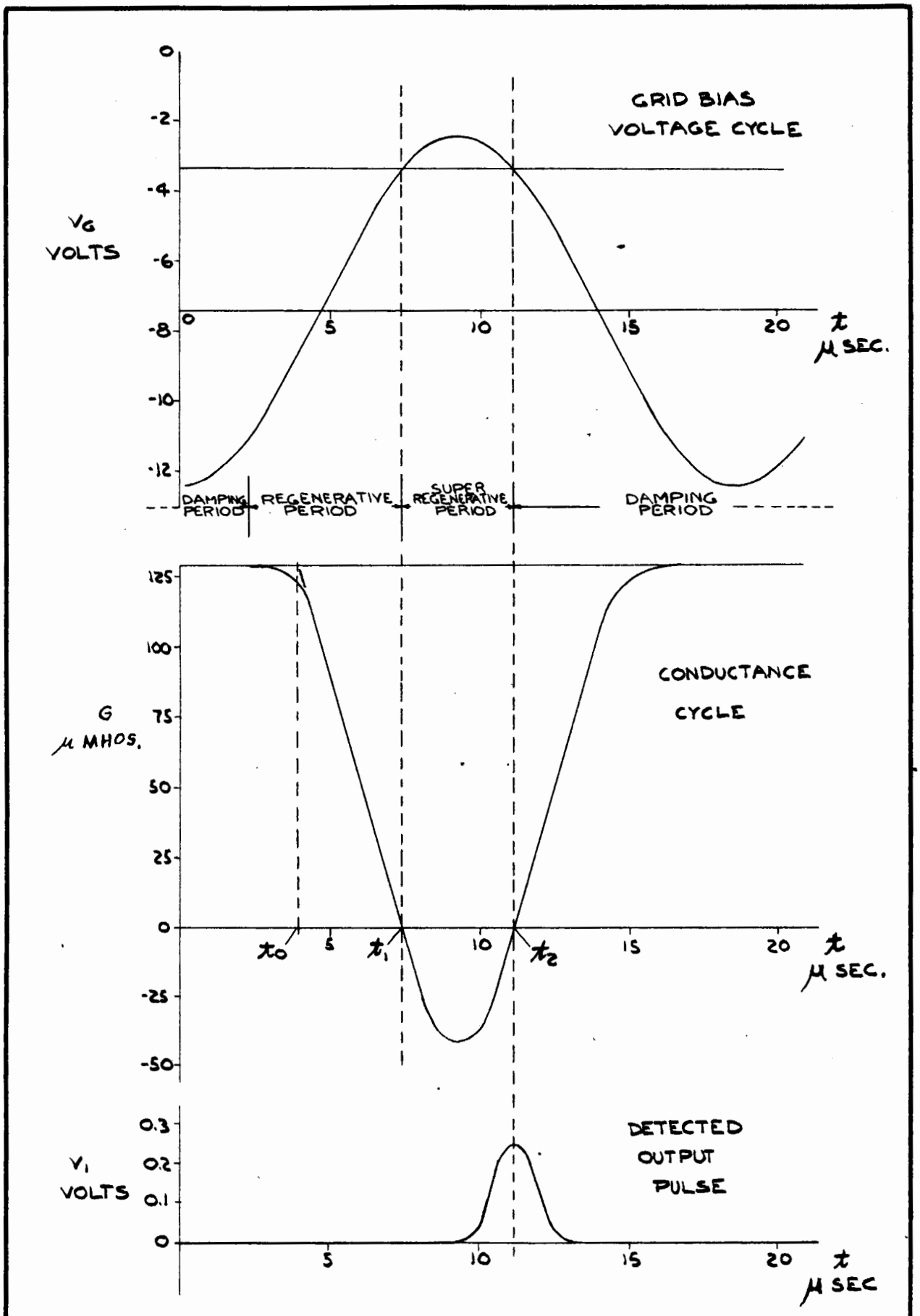


FIG.3.6 DETERMINATION OF THE CONDUCTANCE CYCLE

$$V_1(t) = V_s G_0 \left[\frac{\pi}{C G'(t_1)}\right]^{\frac{1}{2}} \left(\frac{\omega}{\omega_0}\right) \exp\left[\frac{-C(\omega-\omega_0)^2}{G'(t_1)}\right]$$

$$\times \exp\left[\frac{-1}{2C}\int_{t_1}^{t} G(x)\,dx\right] \sin\left[\omega_0 t + (\omega-\omega_0)t_1\right] \qquad (3.5.1)$$

where $V_1(t)$ = oscillation amplitude at time t

$V_s$ = absolute signal amplitude

$\omega_0 = 2\pi f_0$ = radial frequency of the oscillator

$\omega = 2\pi f$ = radial frequency of the signal

C = capacitance of the plate cavity

$G'(t_1)$ = derivative of the conductance with respect to time at $t = t_1$

The ratio of $V_1$ over $V_s$ can be obtained from above and then greatly simplified when the input signal is tuned to the receiver. It is given by

$$\frac{V_1(t)}{V_s} = G_0 \left[\frac{\pi}{C G'(t_1)}\right]^{\frac{1}{2}} \exp\left[\frac{-1}{2C}\int_{t_1}^{t} G(x)\,dx\right] \qquad (3.5.2)$$

where the sinusoidal variation with time is also left out.

For $t = t_2$ the oscillation amplitude $V_1$ is simply the peak of the output pulse and $-\int_{t_1}^{t_2} G(x)\,dx$ becomes $a^-$ as was defined previously. The last equation then reduces to

$$\frac{V_1(t_2)}{V_s} = G_0 \left[\frac{\pi}{C G'(t_1)}\right]^{\frac{1}{2}} \exp\left[\frac{a^-}{2C}\right] \qquad (3.5.3.)$$

which can be rewritten so as to get an expression for $a^-$, namely

$$a^- = 2C \ln\left[\left[\frac{C G'(t_1)}{\pi}\right]^{\frac{1}{2}} \frac{V_1(t_2)}{V_s G_0}\right] \qquad (3.5.4.)$$

$$= 114\ \mu\text{mhos.}\,\mu\text{sec.}$$

which compares favourably with 105 $\mu$mhos.$\mu$sec. from the graphical method. Judging from the reading accuracy in conducting the various measurements, it is estimated that the value of C is known to within $\pm$ 20% and that of b is known to within $\pm$ 10%. The possible error for $a^-$ is about 20%, since most of its contribution comes from the C outside the logarithm in equation (3.5.4.).

The discrepancy in the two values of $a^-$ is well within this error.

An expression for the total receiver gain $N_t$ can be obtained from equation (3.5.3.) by taking the natural logarithms of both sides. This gives

$$N_t = \ln\left[\frac{V_1(t_2)}{V_s}\right]$$

$$= \ln\left[G_o\left[\frac{\pi}{C\,G'(t_1)}\right]^{\frac{1}{2}}\right] + \frac{a^-}{2C}$$

$$= N_o + N_s \text{ nepers} \qquad (3.5.5.)$$

so that $$N_o = \ln\left[G_o\left[\frac{\pi}{C\,G'(t_1)}\right]^{\frac{1}{2}}\right] \text{ nepers} \qquad (3.5.6.)$$

and $$N_s = \frac{a^-}{2C} \text{ nepers} \qquad (3.5.7.)$$

$N_o$ is called the slope gain. It is the contribution to the total gain that occurs during the regenerative period, when the net conductance across the resonant circuit is positive but is dropping to zero. $N_s$ has already been mentioned before and is called the super-regenerative gain, since it acts during the super-regenerative period. $N_o$ works out to be 2.62 nepers or 22.8 db and $N_s$, as obtained graphically, is 6.65 nepers or 57.0 db. Under normal operating conditions the mean grid bias voltage may be much smaller, in which case the super-regenerative period would be longer and the regenerative period shorter. That would be accompanied by a larger $N_s$ and smaller $N_o$.

There were several conditions which had to be met in order that equation (3.5.1.) be valid. Firstly, it is a formula for the slope-controled state and the requirement for slope control is that

$$t_1 - t_o > \frac{12C}{G_o} \qquad (3.5.8.)$$

where $t_o$ is defined in fig. 3.6. It is found that

$$t_1 - t_o = 3.5\,\mu\text{sec.} \qquad (3.5.9.)$$

and $$\frac{12C}{G_o} = 0.73\,\mu\text{sec.} \qquad (3.5.10.)$$

which satisfy the condition stated in equation (3.5.8.).

The oscillation amplitude is actually obtained as the sum of two parts, of

which $V_1$ is the more important term if the condition for slope control is satisfied and that

$$t_2 - t_o > t_1 - t_o \qquad (3.5.11)$$

The first condition has been met and the second is also satisfied from knowing that

$$t_2 - t_o = 3.7\,\mu\text{sec.} \qquad (3.5.12)$$

and from equation (3.5.9).

## 3.6 Super-regenerative band-width

Equation (3.5.1) shows how the super-regenerative oscillator reacts to frequencies other than that of the receiver. The frequency response $S(f)$ can be described by

$$S(f) = \frac{\omega}{\omega_o} \exp\left[\frac{C(\omega-\omega_o)^2}{G'(t_1)}\right]$$

$$= \frac{f}{f_o} \exp\left[\frac{-4\pi^2 C (f-f_o)^2}{G'(t_1)}\right] \qquad (3.6.1)$$

which behaves like a Gaussian error-curve for f not far too different from $f_o$; The band-width $b_s = 2(f-f_o)$ is obtained approximately when

$$\exp\left[\frac{-4\pi^2 C (f-f_o)^2}{G'(t_1)}\right] = \exp[-1] \qquad (3.6.2)$$

$$\text{or} \quad b_s = \frac{1}{\pi}\left[\frac{G'(t_1)}{C}\right]^{\frac{1}{2}} \text{ nepers} \qquad (3.6.3)$$

Fig. 3.7 gives the relative response of the receiver in db. The band-width $b_s$ is measured at -8.7 db. to be 0.63 Mc./sec. The expected band-width from equation (3.6.3.) is

$$b_s = \frac{1}{\pi}\left[\frac{34.4}{7.9 \times 10^{-12}}\right]^{\frac{1}{2}}$$

$$= 0.66 \text{ Mc./sec.}$$

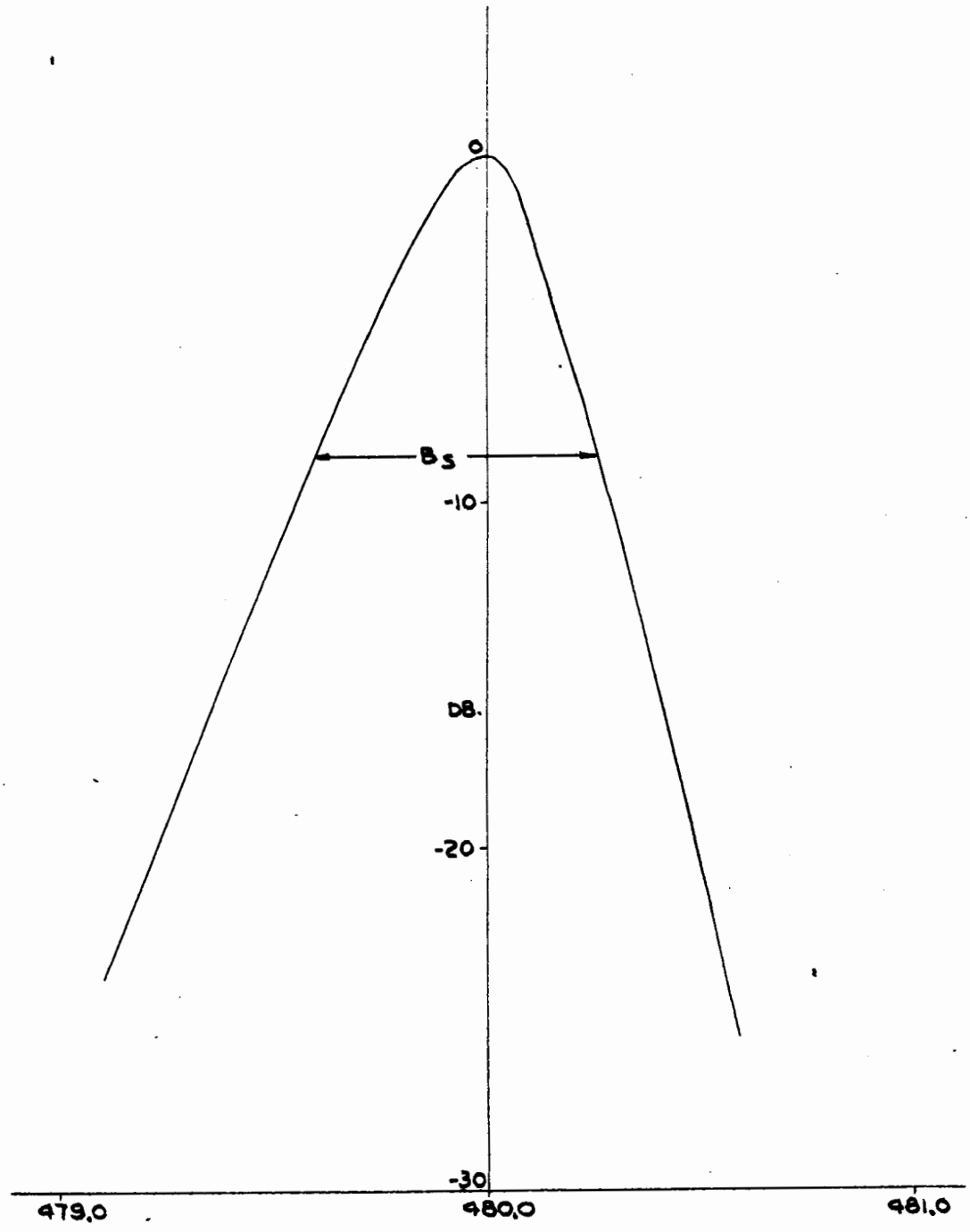


FIG. 3.7 RELATIVE FREQUENCY RESPONSE OF THE RECEIVER

which compares very well with the experimental value.

The energy band-width for noise calculations is defined as

$$b_{ms} = \frac{1}{S(f_o)^2} \int_{-\infty}^{+\infty} |S(f)|^2 \, df$$

where the experimental results of $|S(f)|^2$ are given in fig. 3.8. Since $S(f_o) = 1$, the area under the curve, which is just the integral, gives the band-width. This is illustrated by means of a rectangle having a height equal to unity and a width equal to the band-width, which turned out to be 0.38 Mc./sec.

## 3.7 Noise figure

The performance of the receiver must be compared with an ideal receiver with respect to noise. For normal purposes it is only possible to receive signals in a band whose width equals the quench frequency $f_q$ so that the ideal comparison receiver must have a band-width $f_q = 54$ Kc./sec. also.

The noise generated in a 54 Kc./sec. band-width is

where K = Bottzman's constant $1.37 \times 10^{-23}$ joules/$^\circ$K

T = Temperature of the resistance in degrees Kelvin

R = Internal resistance of the source in ohms.

f = Receiver noise band-width in cycles/sec.

It was necessary to determine the amount of noise present in the receiver. A 100% amplitude modulated signal was fed to the receiver and the signal amplitude was decreased until the peak noise level in the valleys of the

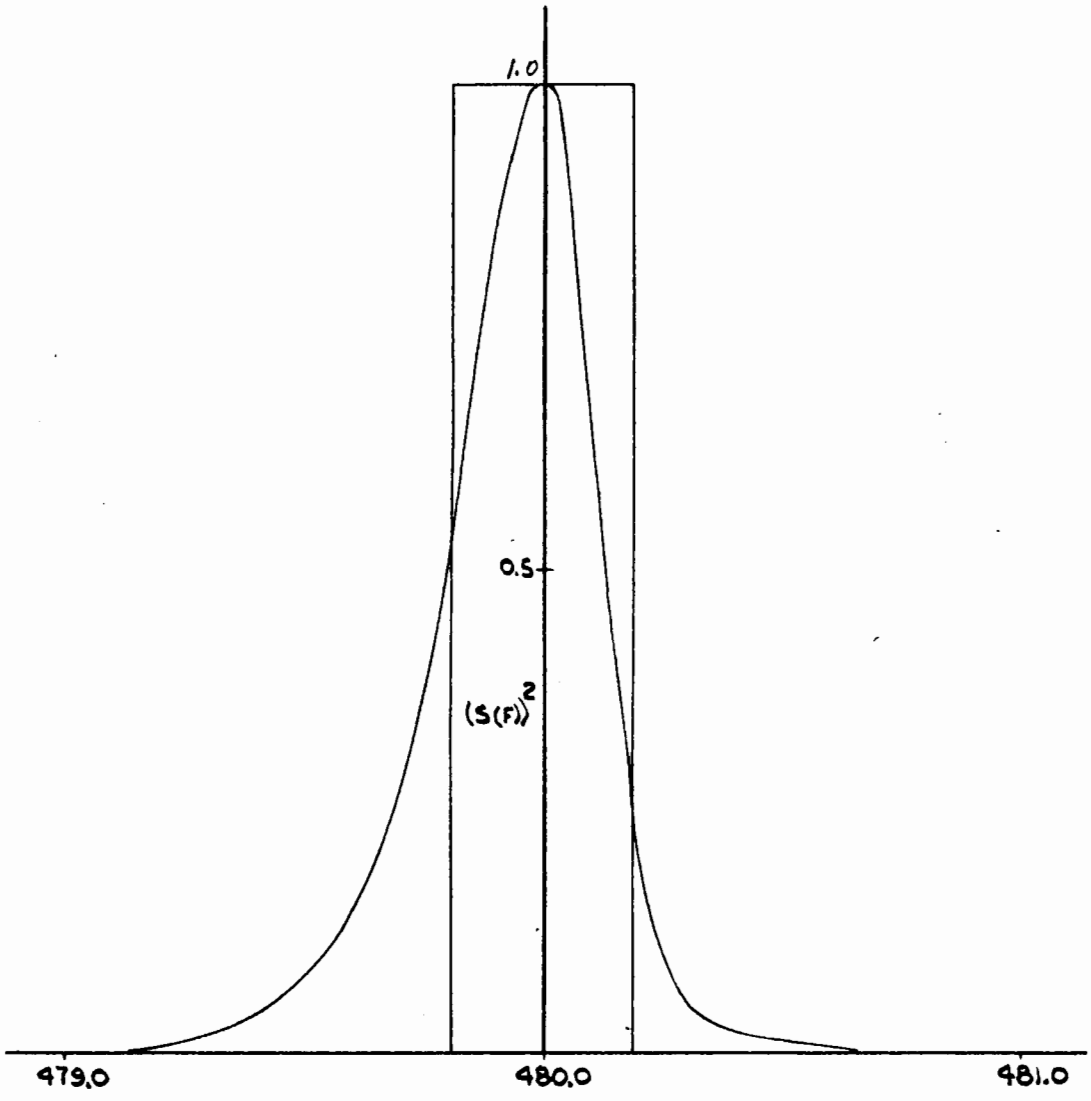


FIG. 3.8 NOISE BAND-WIDTH MEASUREMENT

modulation rose to the mean carrier level. The r.m.s. carrier voltage was 3.0$\mu$v. which indicated that the "1% level" had a value of 4.24$\mu$v. If we assume what happens to be the peak value of noise as the level which is exceeded for 1% of the time, this level is 2.33 x r.m.s. value, thus giving 1.82$\mu$v. for the r.m.s. noise.

Now $1 + \frac{l_s}{l_t} = 10$

and the approximate noise figure $= 20 \times \log_{10} 10 = 20$ db

It has been shown by H.A. Wheeler that the noise figure of a super-regenerative receiver is larger than that of a straight amplifier, having the same band-width, by a factor which equals

$$b_s/f_q$$

where $b_s$ = the super-regenerative band-width

and $f_q$ = the quench frequency

The reason for this is that the super-regenerative receiver is sensitive to noise in a band equal to $b_s$, but it beats with the component frequencies of the general spectrum and appears in a band whose width equals the quench frequency $f_q$.

The ratio can be worked out and is

$$\frac{b_s}{f_q} = \frac{650 \times 10^3}{54 \times 10^3}$$

$$= 12.0 \text{ or } 11 \text{ db.}$$

Subtracting from the noise figure the value of this ratio, you obtain 9 db, which is a reasonable noise figure for the 5876 triode alone in a first-class conventional circuit.

## 3.8 Oscillograms of oscillator pulses

The 500 Mc./sec. oscillations leave the oscillator in the form of pulses at quench frequency. These pulses are detected and observed on an oscilloscope.

Fig. 3.9a shows the random noise output when no signal is present, while in fig. 3.9b one can see the superimposed output pulses for only noise at the receiver input. The pulses have a Gaussian waveform and a wide distribution in amplitude corresponding to the wide amplitude variation of the noise at the input. Fig. 3.10a shows the detected output for a large, continuous wave signal at the input, with fig. 3.10b giving the constituent superimposed pulses. These are all of the same amplitude and hence the trace appears as a solid line. One can observe how the pulse resembles a Gaussian waveform, as had been predicted by theory.

Fig. 3.11 illustrates how the pulses form an amplitude modulated sine wave. In fig. 3.11a is shown a linearly amplified output of a signal whose amplitude was modulated with 1 Kc./sec. In the next picture, one can see the individual pulses, of which it takes 54 to reproduce one wavelength. The third picture shows the relative separation of the pulses and fig. 3.11d gives the pulses all superimposed. There are sharp limits at the top and bottom which correspond to the pulses describing the top and bottom peaks of the amplitude modulated signal.

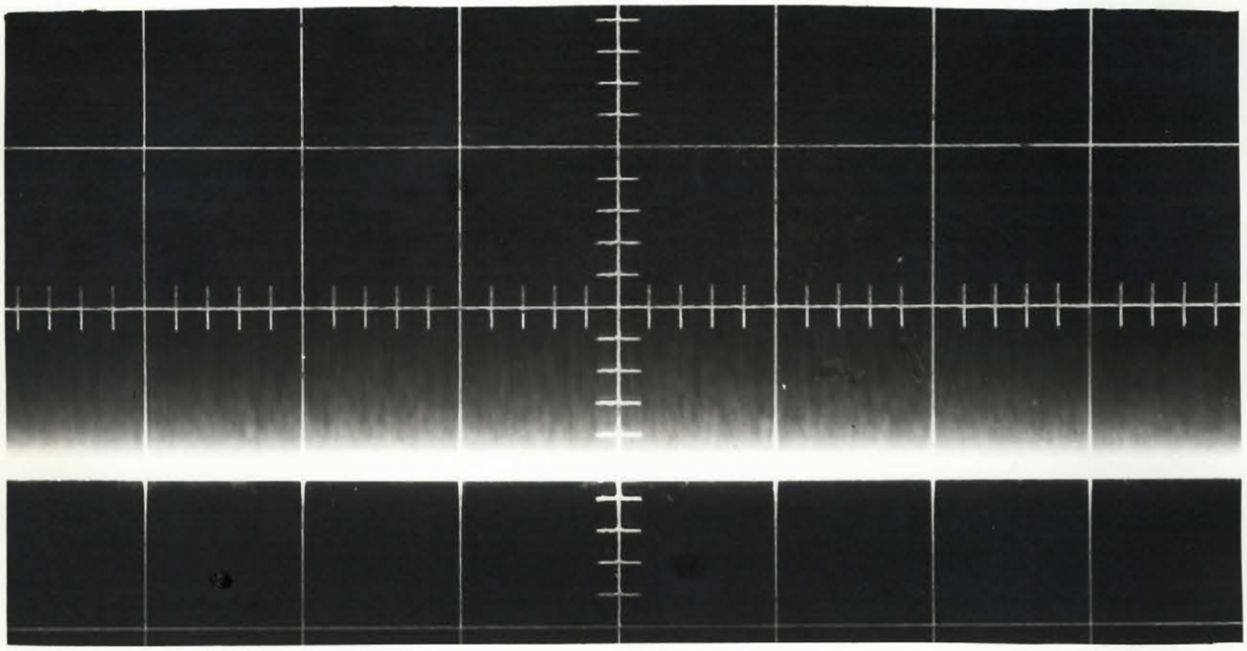

FIG 3.9 (a) OUTPUT NOISE FOR NO INPUT SIGNAL

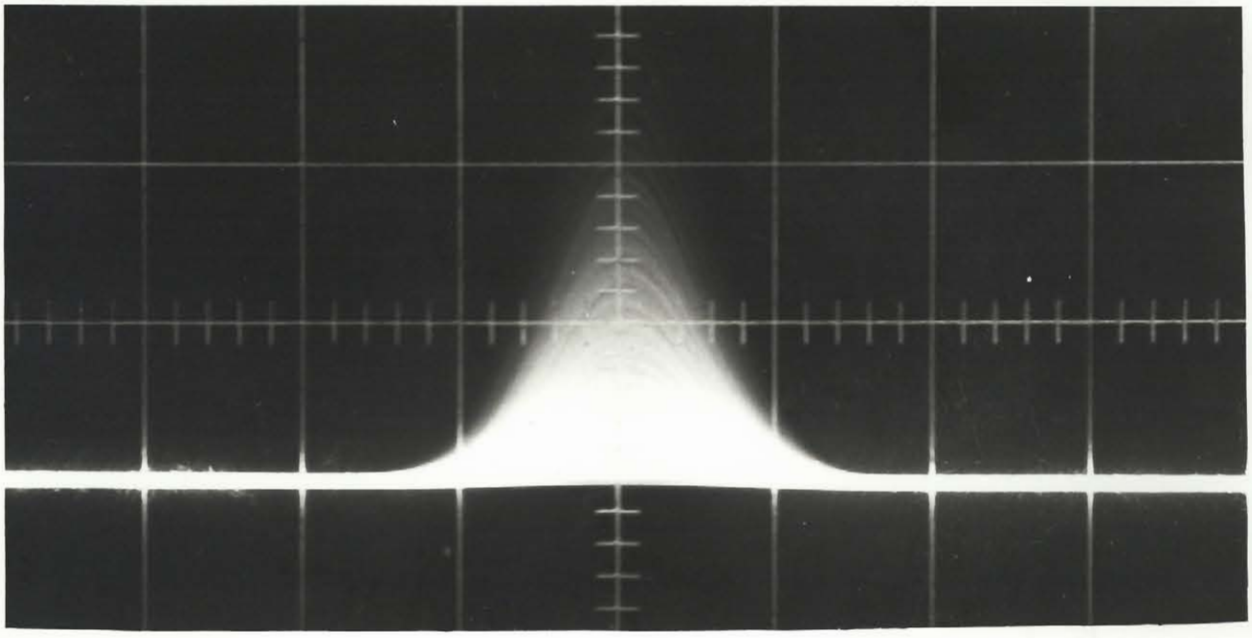

FIG. 3.9 (b) DETECTED PULSES WHICH FORM THE NOISE

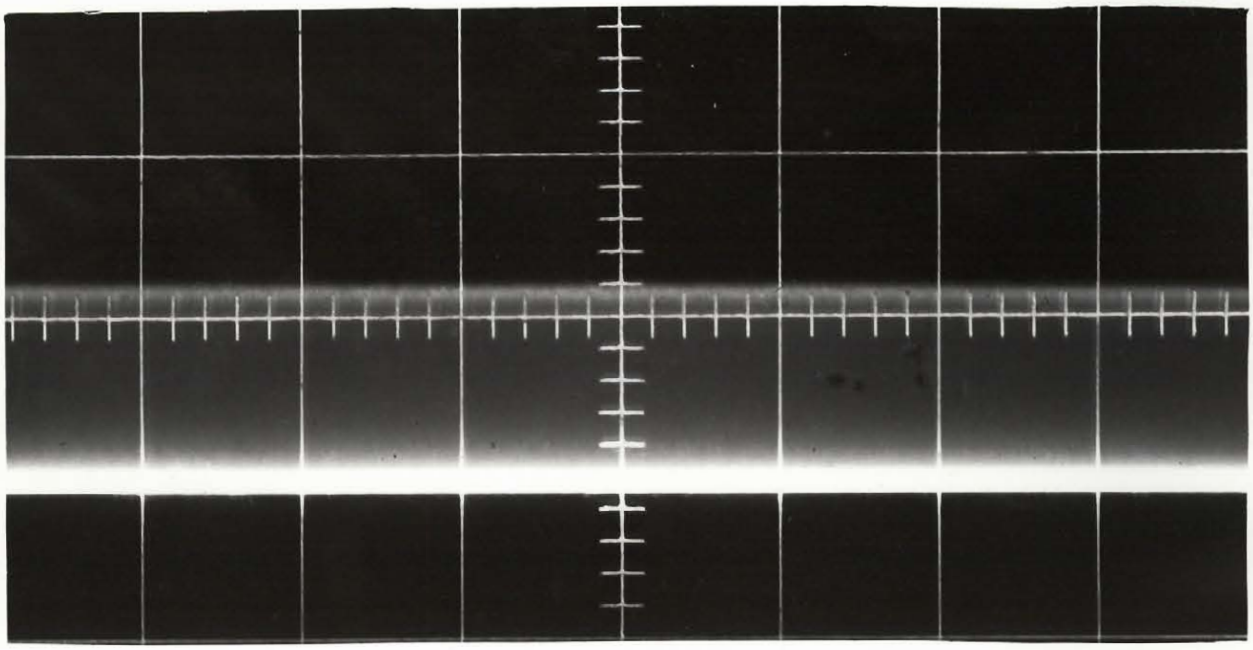

FIG 3.10 (a) OUTPUT FOR LARGE INPUT SIGNAL

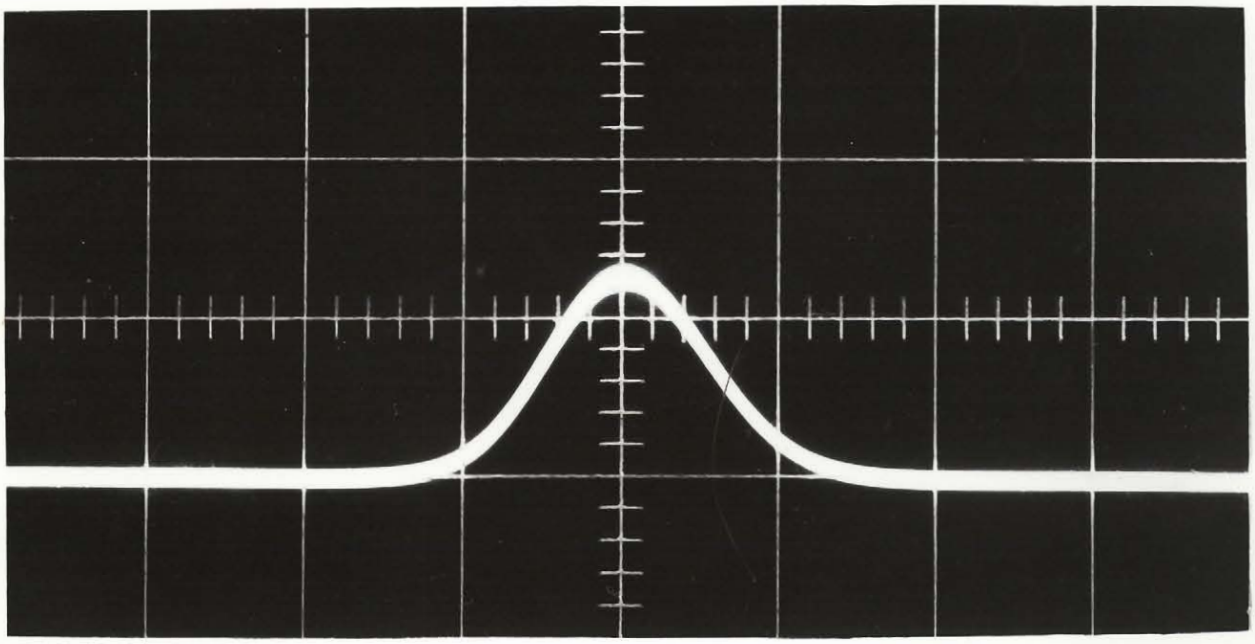

FIG 3.10 (b) SUPERIMPOSED OUTPUT PULSES OF EQUAL AMPLITUDE

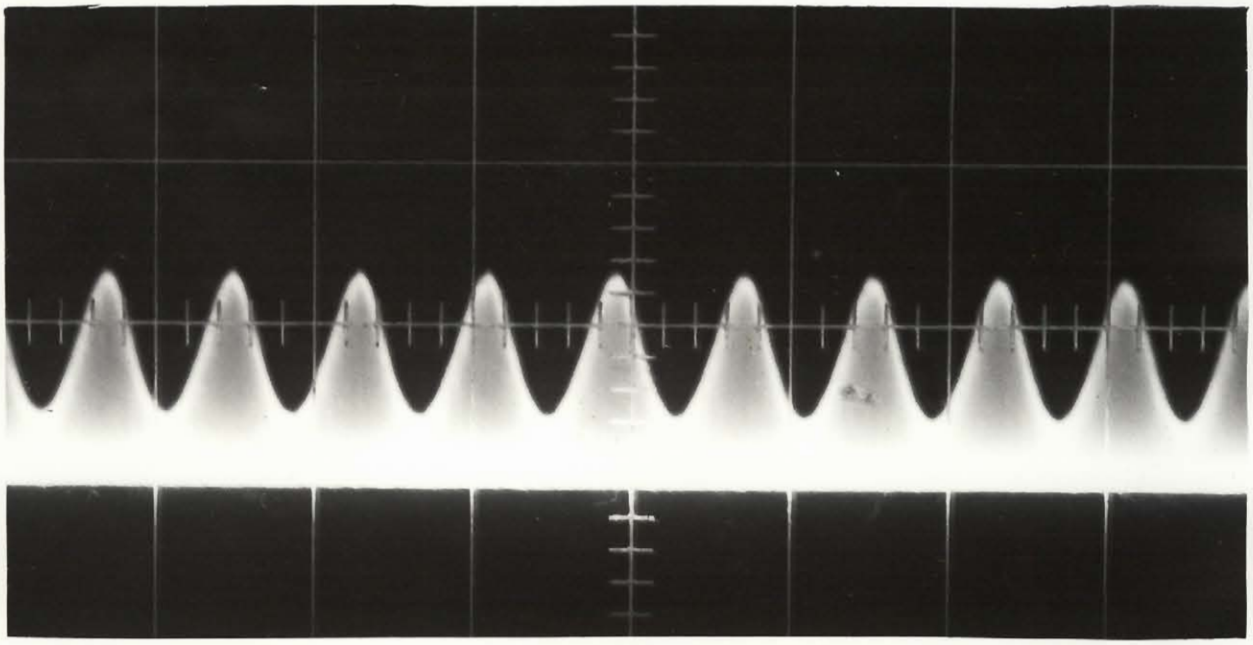

FIG 3.11(a) OUTPUT FOR AN AMPLITUDE MODULATED INPUT SIGNAL

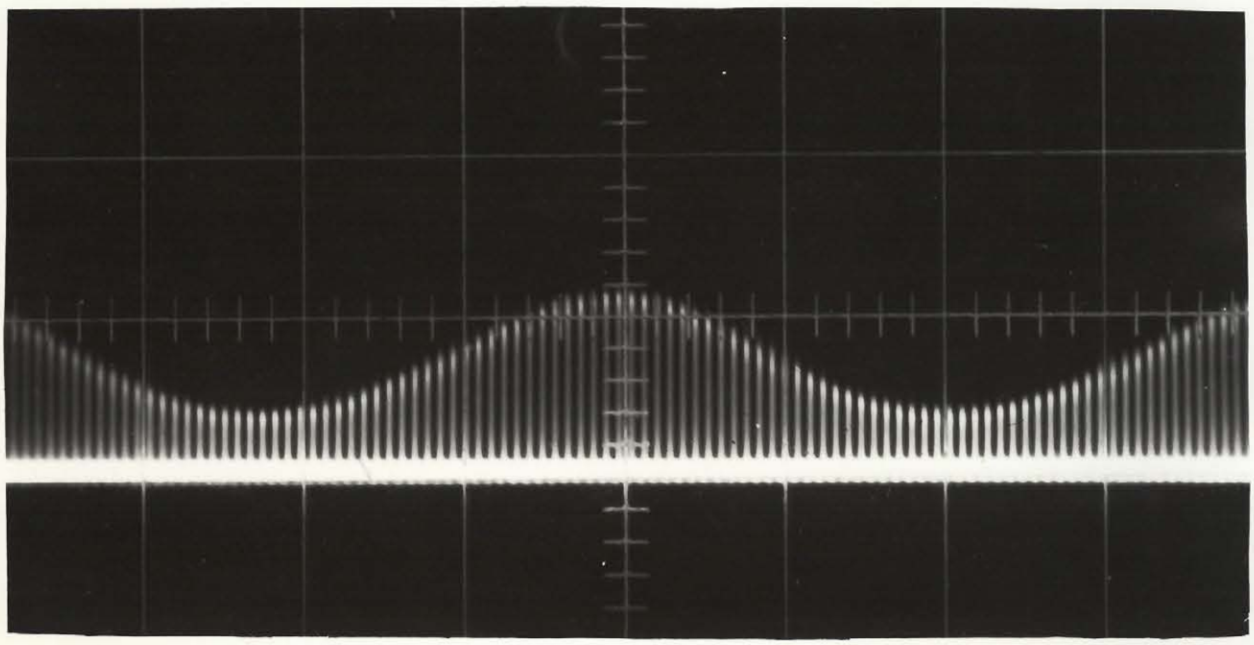

FIG 3.11(b) FORMATION OF THE SINE WAVE

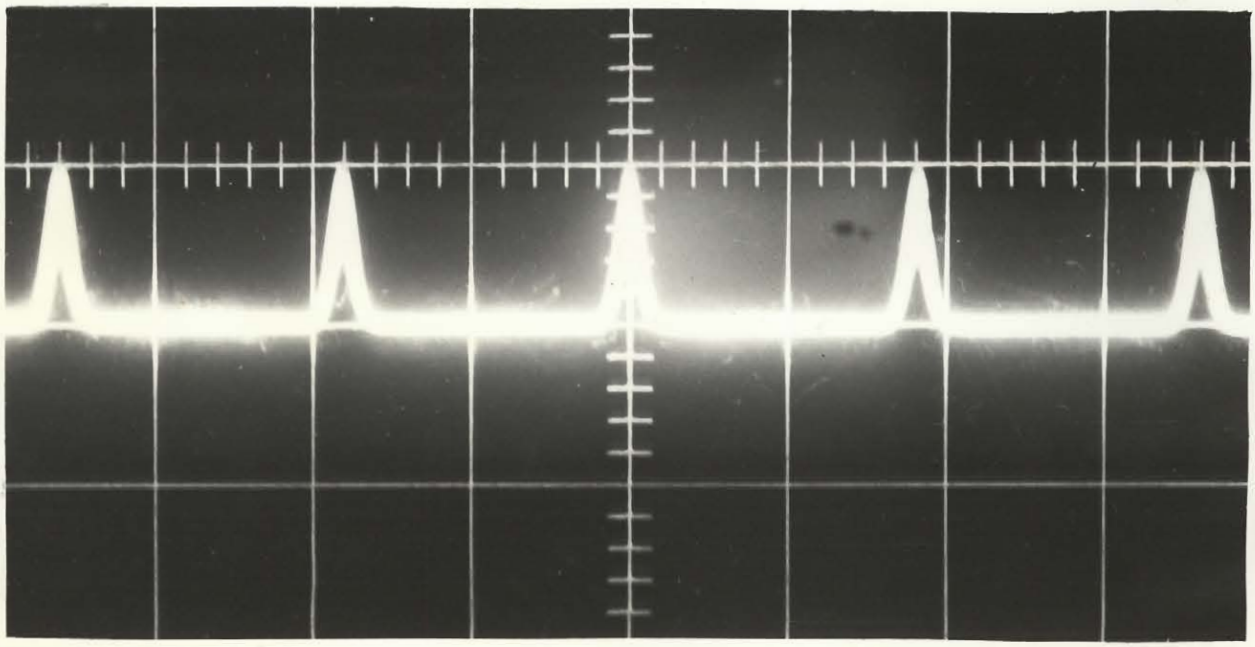

FIG 3.11 (c) RELATIVE SEPARATION OF THE PULSES

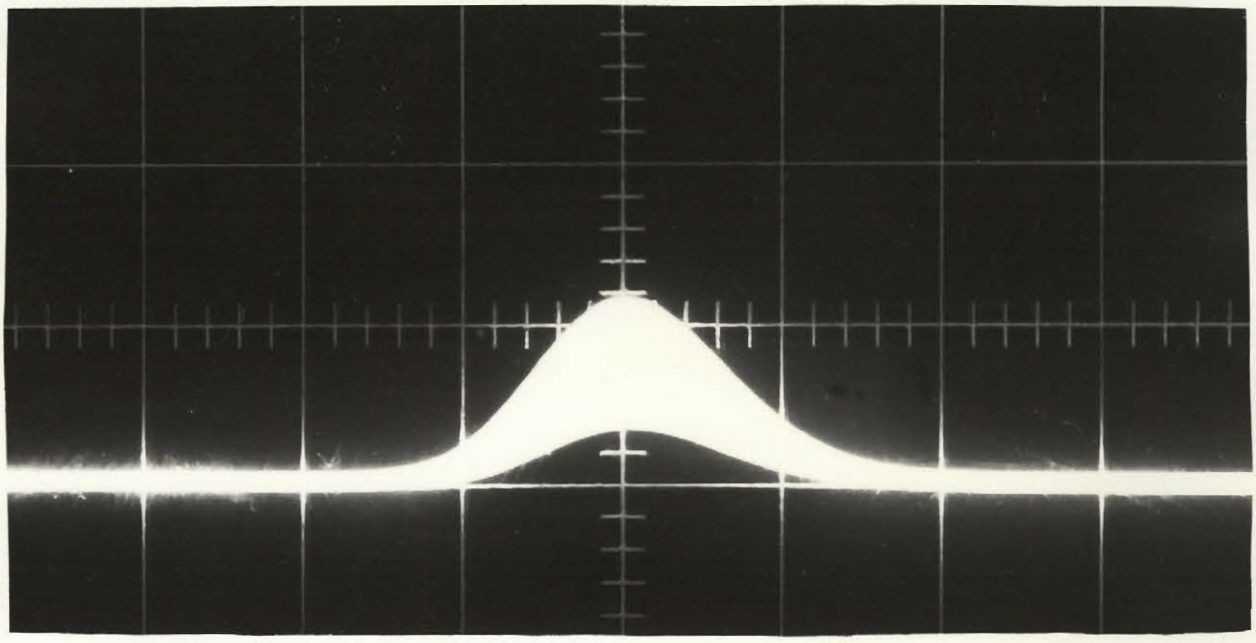

FIG 3.11 (d) SUPERIMPOSED PULSES FOR THE WAVEFORM OF FIG 3.11(a)

# 4. OTHER SECTIONS WHICH CONSTITUTE THE RECEIVER

## 4.1 The quench oscillator

As had been mentioned before, the quench oscillator voltage modulates the u.h.f. oscillator bias voltage. The frequency can be varied from 44 Kc./sec. to 58 Kc./sec. and normally operates near 50 Kc./sec. The oscillator is of the bridge type, being a modification of the Wien type. The frequency determining network is shown in fig. 4.1. $e_i = (e_f - e_r)$ and $e_o$ are the input and output voltage to the amplifies. The ratio of $e_f$ to $e_o$ is given by

$$\frac{e_f}{e_o} = \frac{1}{1 + \frac{C_g}{C_q} + \frac{C_g R_s}{C_q R_p} + j\omega C_g R_s + \frac{1}{j\omega C_q R_p}} \qquad (4.1.1)$$

$$= \frac{1}{1 + \frac{C_g}{C_q} + \frac{C_g R_s}{C_q R_p}} = \frac{1}{3}$$

$$\text{if } C_g = C_q \;,\; R_s = R_p \;,\; \omega_q = \frac{1}{C_g R_s}$$

$$\text{also } \frac{e_r}{e_o} = \frac{R_L}{R_L + R_q} = \frac{1}{K}$$

$$\text{Therefore } e_o = A e_i = A(e_f - e_r)$$

$$\text{or } 1 = A\left(\frac{e_f}{e_o} - \frac{e_r}{e_o}\right)$$

$$= A\left(\frac{1}{3} - \frac{1}{K}\right)$$

It is, therefore, necessary to make K greater than 3 and to have no phase shift (no imaginary part in A) at resonant frequency. A diagram of the circuit is shown in fig. 4.2. The 3 watt tungsten lamp R is a non-linear arm of the bridge and accounts for the stable oscillations. Its temperature is high enough to prevent instability.

$R_P$ acts as a grid leak and $R_L$ as a cathode bias resistor. $C_4$ and $R_4$ decouple the quench oscillator from the rest of the circuit. It was also important to shield the oscillator from the a.g.s., which is tuned to the detected quench frequency pulses from the super-regenerative oscillator. The band-width of the tuned amplifier stage in the a.g.s. is 2 Kc./sec., a maximum drift of

FREQUENCY BRIDGE
OF THE QUENCH OSCILLATOR

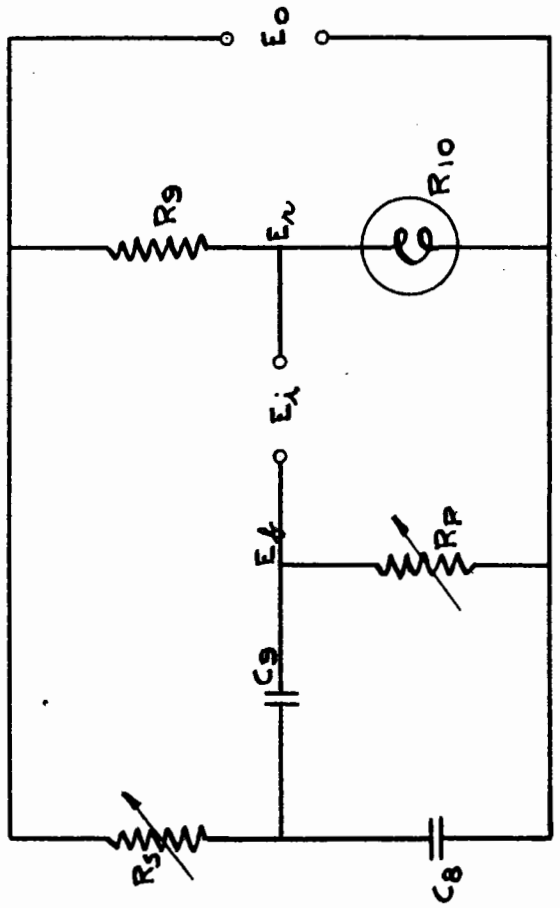


FIG. 4.1

# QUENCH OSCILLATOR

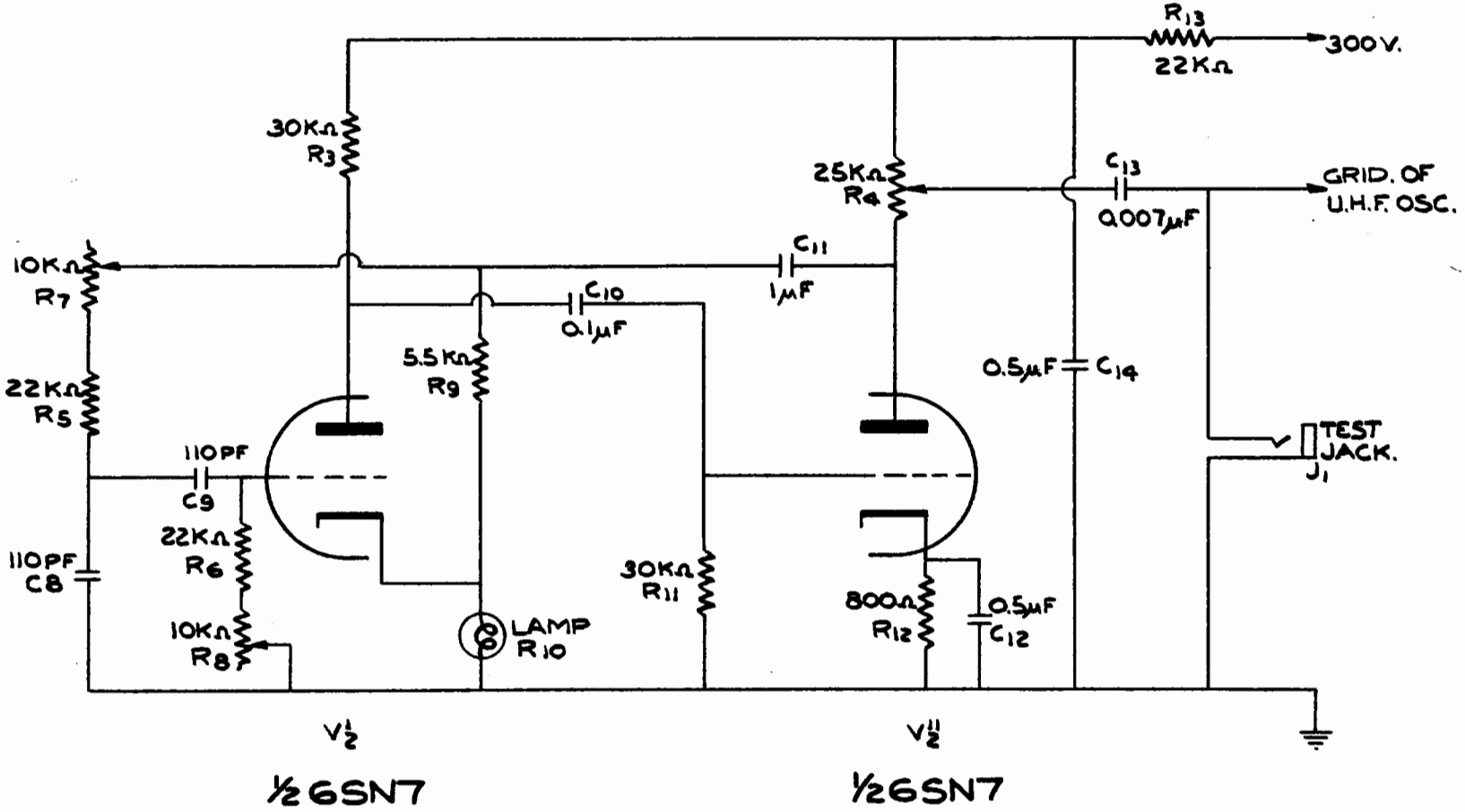


FIG. 4.2

## QUENCH OSCILLATOR

### List of Components

| | | |
|---|---|---|
| $V_2', v_2''$ | 6SN7 | double triode |
| $R_3$ | 30K Ω | |
| $R_4$ | 25K Ω | 2 watt polentiometer |
| $R_5$ | 22K Ω | 1% tolerance |
| $R_6$ | 22K Ω | 1% tolerance |
| R7 | 10K Ω | potentiometer ) ganged together |
| $R_8$ | 10K Ω | potentiometer ) |
| $R_9$ | 5.5K Ω | |
| $R_{10}$ | 3 watt lamp (non-linear resistance) | |
| $R_{11}$ | 30K Ω | |
| $R_{12}$ | 800 Ω | |
| $R_{13}$ | 22K Ω | |
| $C_8$ | 110 pf. | 1% tolerance |
| $C_9$ | 110 pf. | 1% tolerance |
| $C_{10}$ | 0.1 μf. | |
| $C_{11}$ | 1 μf. | |
| $C_{12}$ | 0.5 μf. | |
| $C_{13}$ | 0.007 μf. | |
| $C_{14}$ | 0.5 μf. | |
| $J_1$ | test jack | |

1 Kc./sec. or 2% can be tolerated in the quench frequency, which is given by $1/2\pi R_s C_9$ . $R_s$ consists of a fixed 22 K$\Omega$ resistor in series with a fraction of an Ohmite 10 K$\Omega$ potentiometer. The major variation in $R_s$ will be due to temperature changes, whereas $C_9$ has a zero temperature coefficient. $R_s$ will not change by more than -0.02% per $^{o}$C rise. For a 20$^{o}$C change from the normal operating temperature only 0.4% change would be observed in the frequency, which is well within the a.g.s. band-width.

A maximum amplitude of 25 volts peak can be fed into a 7K$\Omega$ load with very little distortion in the waveform. Almost no distortion exists for an output of less than 5 volts.

## 4.2 The u.h.f. detector and a.g.s. system

A schematic diagram of the circuit is shown in fig. 4.3.

The output pulses from the u.h.f. oscillator are detected by a IN 54 A germanium diode and fed into a tuned amplifier. The tuned amplifier has a toroid and a capacitor $C_{16}$ for the tuned circuit and $R_4$ as a damping resistance to obtain a band-width of 2 Kc./sec., $R_4$ (47K$\Omega$) reduces the Q of the plate load from 45 to 27, thus decreasing the equivalent damping resistance from 30.5 K$\Omega$ to 18.5 K$\Omega$. The amplification at resonance is given by

$$G_m \frac{\omega_q L_1 Q}{1 + \frac{\omega_q L_1 Q}{R_P} + \frac{\omega_q L_1 Q}{R_{20}}}$$

$$= G_m \omega_q L_1 Q \quad \text{approximately}$$

$$= 30$$

The measured amplification was found to be 28 which is in close agreement with theory. It was necessary to decouple the tuned amplifier from the other stages in order to reduce the feedback through the $B^+$ supply, which had originally reduced the gain of the tuned amplifier to 23 and sometimes even maintained oscillations.

# U.H.F. DETECTOR AND AUTOMATIC GAIN STABILIZER

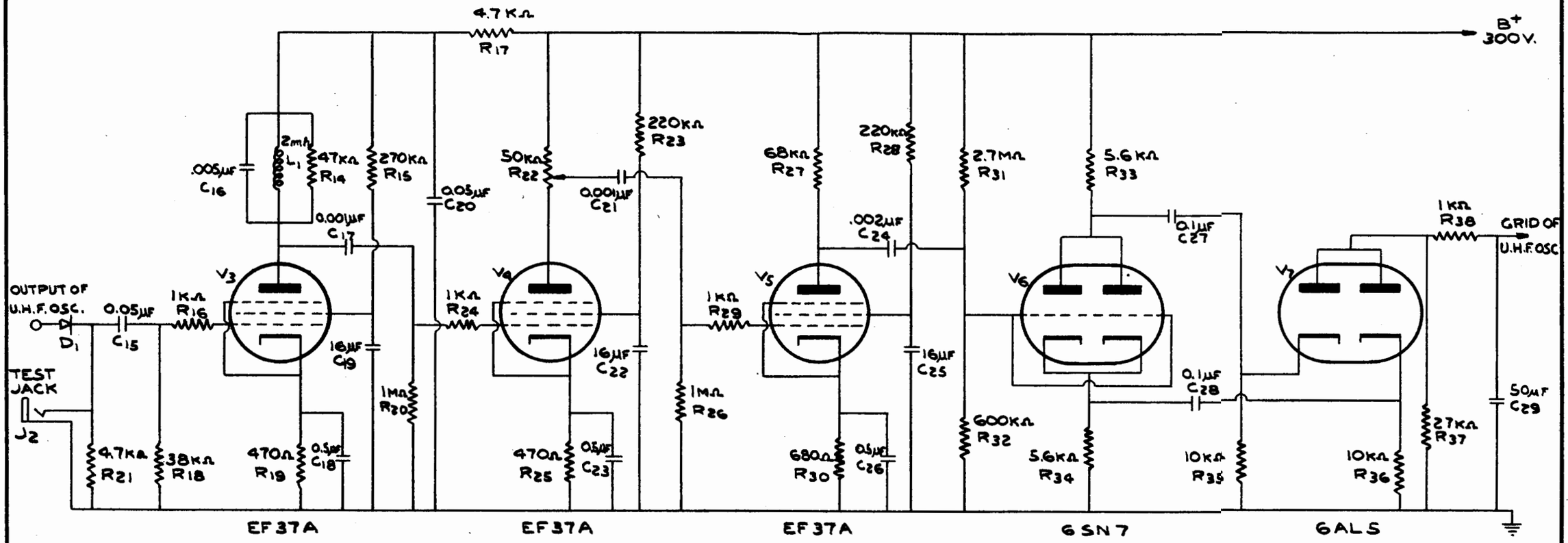


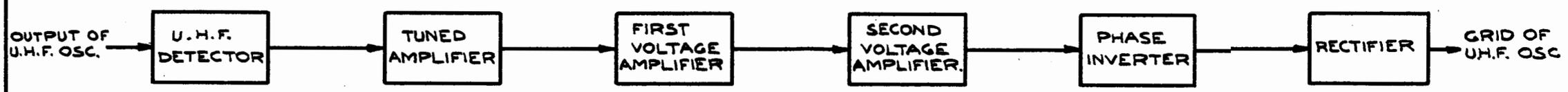


FIG. 4.3

The tuned amplifier was followed by two stages of voltage amplification, each having a gain of about 50 at a frequency of 54 Kc./sec. The gain of the first voltage amplifier was made variable by having a potentiometer for the plate load. The output of the second voltage amplifier fed into the phase inverter whose output impedance, at the plate, equalled $R_{33}$ or 5.6 K$\Omega$ , and at the cathode equalled the reciprocal of the transconductance or 2.3 K$\Omega$ . The values of the components for these sections were chosen from observing the tube characteristics for the EF 37A and the 6SN7. A double diode $V_7$ rectified the 54 Kc./sec. voltage at the plate and cathode of $V_6$ to give out a negative D.C. control voltage for the grid of the u.h.f. oscillator.

In order to satisfy the Nyquist criterion for stability in the feedback loop, it was necessary to introduce a time lag which would be greater than twice the loop gain, multiplied by the sum of the phase lags and delays of the whole loop. This was the reason for the large time constant (0.05 sec.) of $R_{38}$ and $C_{29}$ , and the slow response of the system. By making a rapid increase in signal amplitude at the input of the receiver, it was possible to see a large pulse for a fraction of a second at the crystal IN 54A before the control of the a.g.s. was restored.

For the u.h.f. oscillator to always operate in the linear mode, the requirement on the a.g.s. is simply to have enough gain so that for the largest input signal the oscillations do not reach saturation. It is obvious that, if the input signal is decreased, the output pulses can not increase and so the oscillator can never find itself in the logarithmic mode.

## 4.3 The meter circuit

A circuit showing the meter connections is given in fig. 4.4. $V_8$ is a double rectifier, being similar in operation to $V_7$, but giving out a positive voltage instead. For position 3 of the two-pole six-position switch, one

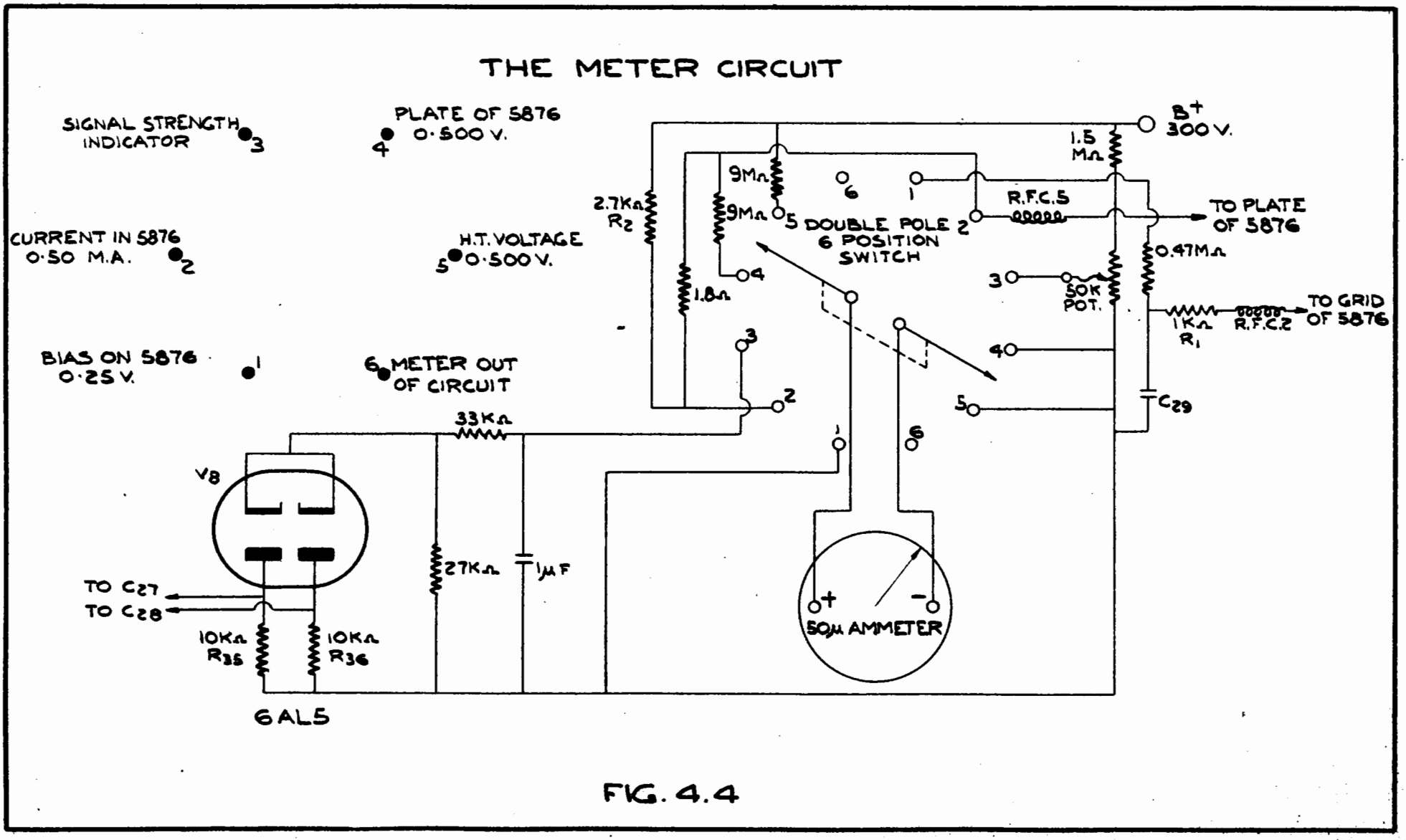
THE METER CIRCUIT
SIGNAL STRENGTH INDICATOR
3
PLATE OF 5876
0·500 V.
4
B+
300 V.
1.5 MΩ
9MΩ
9MΩ
2.7KΩ
R2
6
1
R.F.C.5
TO PLATE OF 5876
5
DOUBLE POLE
6 POSITION
SWITCH
2
CURRENT IN 5876
0·50 M.A.
2
H.T. VOLTAGE
5
0·500 V.
0.47MΩ
4
1.8Ω
3
50K POT.
TO GRID OF 5876
1KΩ
R1
R.F.C.2
BIAS ON 5876
0·25 V.
1
6
METER OUT OF CIRCUIT
3
4
2
5
C29
33KΩ
1
6
V8
27KΩ
1μF
TO C27
TO C28
10KΩ
R35
10KΩ
R36
+
−
50μ AMMETER
6AL5

FIG. 4.4

terminal of the meter is connected to the output of $V_g$ and the other is backed off a variable D.C. voltage with $B^+$ as its source, as shown in fig. 4.4. The 50 K $\Omega$ potentiometer is used as the zero centering of the meter. An external meter can be connected to the jack below the meter, if the panel meter is not sufficiently accurate.

All the other positions of the switch are quite simple. For positions 1, 5 and 6 the meter has a large resistance in series with it and acts like a voltmeter. For position 2, it has a 1.8 $\Omega$ shunt, thus acting like a milliammeter.

The external meter can be used with position 1, 4 or 6 if it has a 55 $\mu$amp. movement and postion 2 if it has a resistance of 1.8 K $\Omega$, and still have the same full scale deflection as the panel meter.

# 5. CONSTRUCTION OF THE RECEIVER

## 5.1 The layout and operation of the receiver

Three views of the receiver are shown in fig. 5.1, 5.2 and 5.3. All the controls are on the front panel with only two test jacks at the rear of the chassis, as seen in fig. 5.2. The waveform of the detected pulses can be observed on the oscilloscope by connecting to the jack labeled "Detected Output Pulses". The output from the other jack gives the quench voltage, which is fed to the grid of the 5876. It enables one to observe the waveform of the quench frequency, measure its amplitude and frequency, as well as to use it as an external trigger for an oscilloscope if one should try to observe the oscillator output pulses.

The two controls on the front panel, for the frequency and amplitude of the quench voltage, are shielded to minimize frequency drift of the quench oscillator. The a.g.s. gain control is not provided with a knob since, after it is set and locked, it does not need resetting very frequently.

The cathode and plate cavities are tuned by means of the two knobs on the front panel and can also be locked if desired, since the tuning shafts are provided with locking nuts. The other controls have already been mentioned in para. 4.4.

## 5.2. The super-regenerative receiver as a "Bridge" detector

A view of the equipment necessary for making measurements with the admittance meter (u.h.f. "Bridge") is shown in fig. 5.4. The signal generator on the right provides the u.h.f. power for the "Bridge", while the receiver at the centre, with its power supply on the left, acts as a detector. The advantage of this type of detector is the fact that, at such high frequencies, the super-regenerative principle is more efficient than the superheterodyne principle.

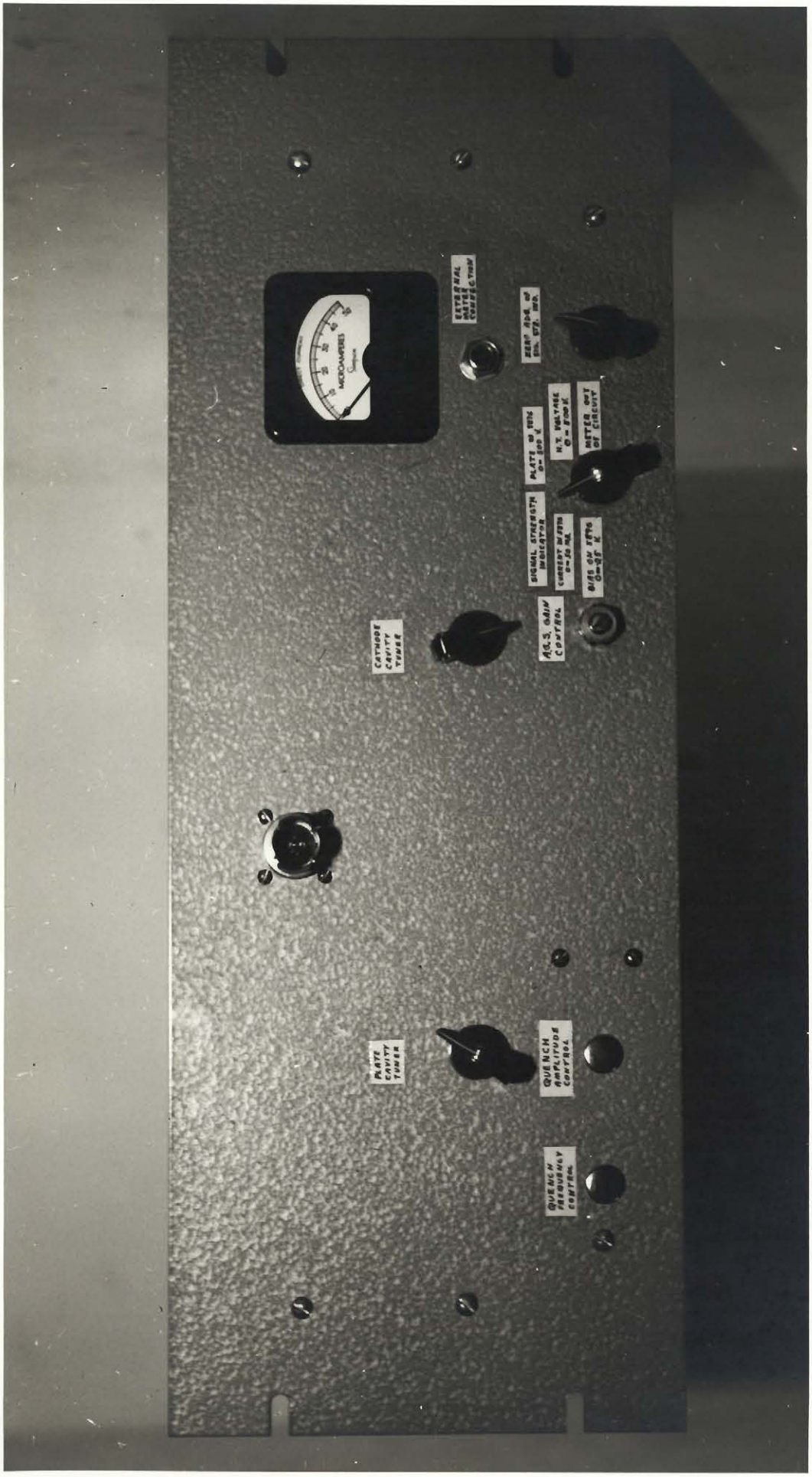


FIG 5.1 RECEIVER, FRONT VIEW


FIG. 5.2 RECEIVER, BACK VIEW

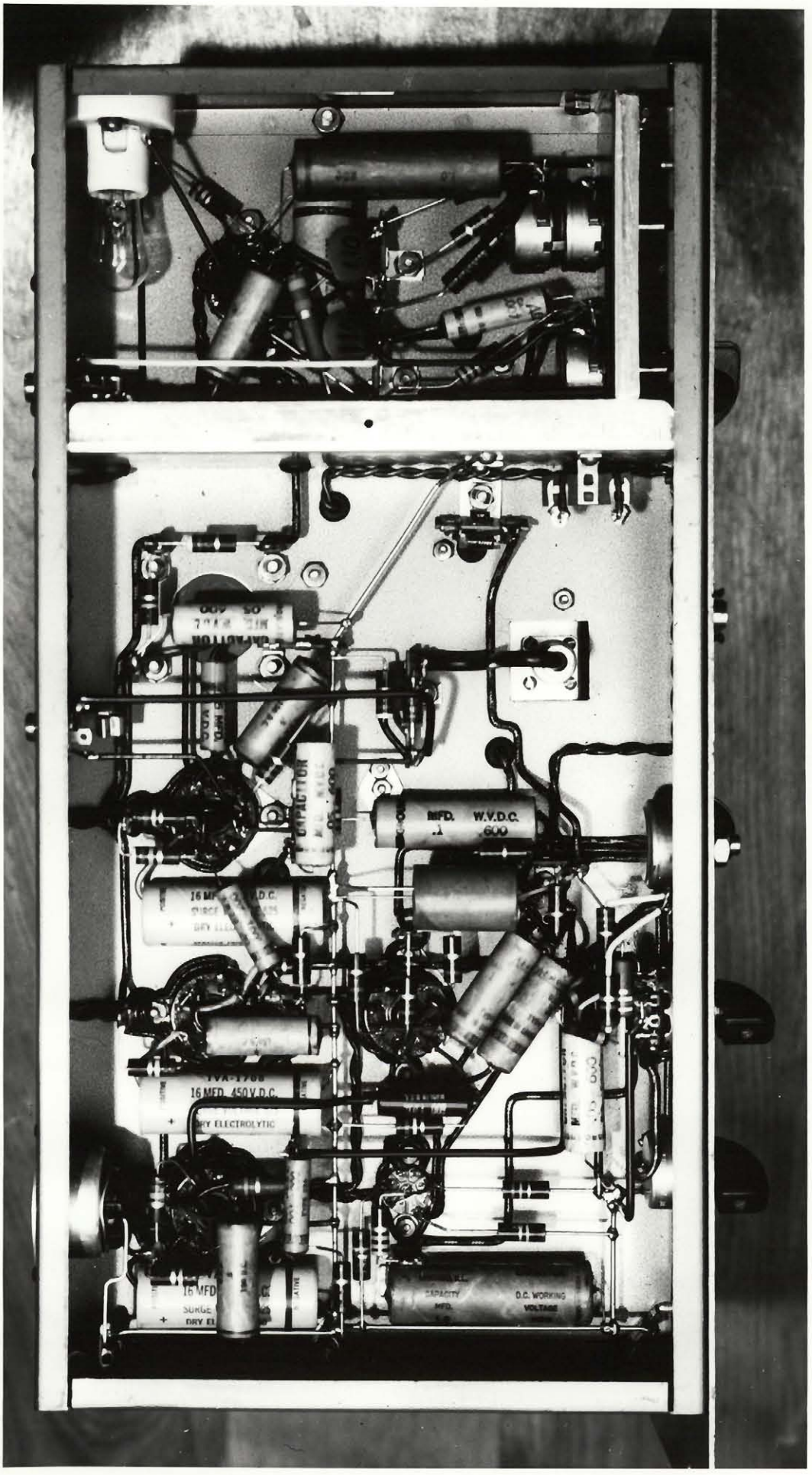


FIG 5.3 RECEIVER, BOTTOM VIEW (WITHOUT SHIELD)

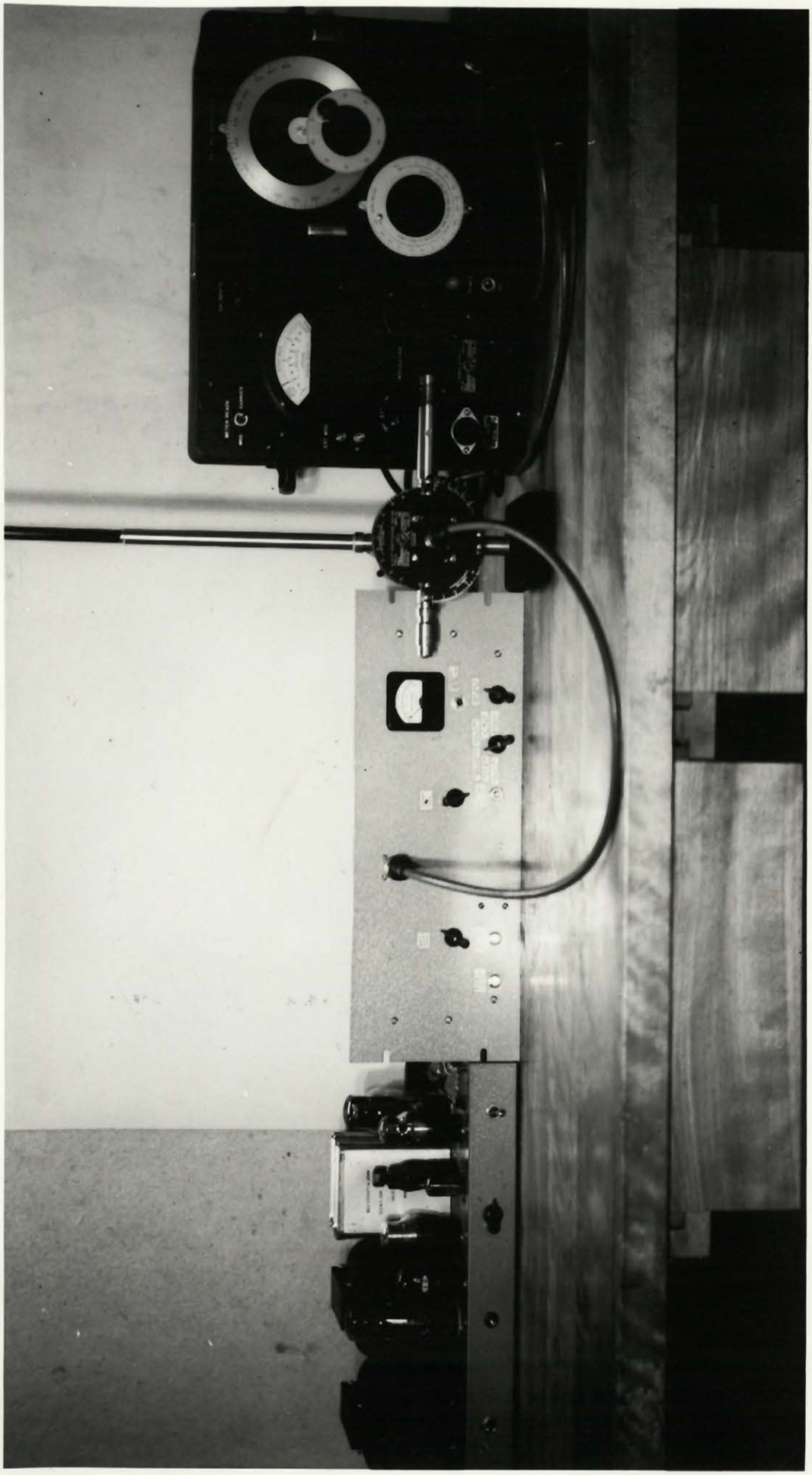

FIG 5.4 "BRIDGE" MEASUREMENT SETUP

The suggested method of detection is to mix the unbalanced signal from the admittance meter with the output of a local oscillator and detect the intermediate frequency with an amplifier. The difficulty lies in finding the desired frequency from the beats of the harmonics. This arrangement has a sensitivity of approximately 5 $\mu$ volts.

It does not compare very well with a sensitivity of 1.5 $\mu$ volts, which is possible with the super-regenerative receiver. The reradiating oscillations of the super-regenerative receiver is of no disadvantage, since their presence is equally felt in all the arms of the admittance meter and does not affect the balance.

# SUMMARY AND CONCLUSIONS

A super-regenerative receiver was designed, and found to be feasible, for operation in a frequency band from 455 Mc./sec. to 510 Mc./sec. The value of $a^-$ was obtained, graphically, to be 105 $\mu$ mhos. $\mu$ sec., while from the formula it turned out to be 114 $\mu$ mhos. $\mu$ sec.

The super-regenerative band-width was measured to be 630 Kc./sec. under normal operating conditions at a general frequency of 54 Kc./sec. and a quench amplitude of 5 volts peak. This result of the band-width was in excellent agreement with the theoretical value of 660 Kc./sec.

The noise figure was determined to be 20 db., of which 11 db. was calculated to be due to the super-regenerative principle, thus leaving 9 db. for the 5876 triode, which is what one would expect from a first class conventional circuit.

The receiver was able to detect 1.5 $\mu$ volts of input signal and hence easily fulfilling the sensitivity requirements for its use as a "bridge" detector.

The receiver is also sufficiently sensitive and stable to be used as a field strength meter. At the "Signal Strength Indicator" position of the switch on the panel, the meter has an approximately logarithmic response. It would be possible to get signal strength directly in db. when the meter is calibrated.

# APPENDIX 1

## The Power Supply for the Receiver

The power supply should have an internal resistance of less than 50 $\Omega$ at D.C and at 54 Kc./sec. In the power supply that was used, there were two filament transformers. One of these with its centre top grounded was used for all the tubes whose cathodes were near ground potential. The other was used for the filament of the 6SN7 phase inverter whose cathode was at a mean potential of 60 volts and a possible peak potential of 120 volts.

The power supply is connected to the receiver through a six conductor cable with an octal socket. The places on the power supply to which the wire are connected can be known by observing the colours of the wires. The connections to the octal socket are numbered below together with the colour of the wire going to each connector.

| | | |
|---|---|---|
| 1. | ground | blue |
| 2. | general filaments | black |
| 3. | $B^+$ 300V | white |
| 4. | not used | - |
| 5. | $V_6$ filament | brown |
| 6. | $V_6$ filament | green |
| 7. | general filaments | red |
| 8. | not used | - |

## REFERENCES


Armstrong, E. H., Some recent developments in regenerative circuits. Proc. Inst. Radio Engrs., N.Y. 10, 244 (Aug. 1922).

Ataka, H., On super-regeneration of an ultra-short wave receiver. Proc. Inst. Radio Engrs., N.Y. 23, 481 (Aug. 1935).

Schroggie, M. G., The super-regenerative receiver. Wireless Engr., 13, 581 (Nov. 1936).

Frink, F. W., The basic principles of super-regenerative reception. Proc. Inst. Radio Engrs., N.Y. 26, 76 (Jan. 1936).

Lewis, W. B. and Milner, C. J., A portable duplex radio telephone. Wireless Engr., 13, 475 (Sep. 1936).

Becker, S. and Leeds, L. M., A modern two way radio system. Proc. Inst. Radio Engrs., N.Y. 24, 1183 (Sept. 1936).

Bradley, W. E., Super-regenerative detection theory. Electronics 21, 96 (Sept. 1948).

Hazeltine, A., Richman, D. and Loughlin, B. D., Super-regenerative design. Electronics p. 99 (Sept. 1948).

Macfarlane, G. G. and Whitehead, J. R., The super-regenerative receiver in the linear mode. F. Instn. Elect. Engrs., 93 Part III A, p. 284 (March-May 1946).

Macfarlane, G. G. and Whitehead, J. R., The theory of the super-regenerative receiver operated in the linear mode. F. Instn. Elect. Engrs., 95 Part III, p. 143 (May 1948).

Glucksman, H. A., Super-regeneration; an analysis of the linear mode. Proc. Inst. Radio Engrs., N.Y. 37, 500 (May 1949).

Whitehead, J. R., Super-Regenerative Receivers, Cambridge University Press (1950).

Wheeler, H. A., Wheeler Monographs, Volume 1, Numbers 3 and 7, Wheeler Laboratories Great Neck, New York (1953).